CHALMERS

# Temperature Controlled Thermal Jacket

## Design and Implementation of a Temperature-Regulated Heated Jacket Prototype

Bachelor's thesis in Electrical Engineering

Edvin Hansson, Moa Johnsson, Marcus Koponen Edvardsson
Alfred Lindell, Caroline Pohjanvuori, Felix Sjöstedt
Group 26

DEPARTMENT OF ELECTRICAL ENGINEERING
CHALMERS UNIVERSITY OF TECHNOLOGY
Gothenburg, Sweden 2025
www.chalmers.se

Bachelor's thesis 2025

# Temperature Controlled Thermal Jacket

Design and Implementation of a Temperature-Regulated Heated Jacket Prototype

Edvin Hansson, Moa Johnsson, Marcus Koponen Edvardsson
Alfred Lindell, Caroline Pohjanvuori, Felix Sjöstedt
Group 26


CHALMERS

Department of Electrical Engineering
*Division of Power Electronics*
Chalmers University of Technology
Gothenburg, Sweden 2025

Temperature Controlled Jacket
Design and Implementation of a Temperature-Regulated Heated Jacket Prototype
Edvin Hansson, Moa Johnsson, Marcus Koponen Edvardsson
Alfred Lindell, Caroline Pohjanvuori, Felix Sjöstedt



Supervisor: Vaishnavi Ravi, Electrical Engineering
Examiner: Jimmy Ehnberg, Electrical Engineering

Bachelor's Thesis 2025
Department of Electrical Engineering
Division of Power Electronics
Chalmers University of Technology
SE-412 96 Gothenburg
Telephone +46 31 772 1000

Cover: Image of developed thermal jacket prototype

Typeset in LaTeX
Printed by Chalmers Reproservice
Gothenburg, Sweden 2025

# Abstract

This bachelor's thesis explores the design and implementation of a temperature-regulated electrically heated jacket prototype. Heat is generated in a nichrome wire when subjected to power from a Lithium Polymer battery. Power delivery is managed through a designed synchronous buck converter. A Proportional–Integral control system is implemented to regulate output voltage and to stabilize the temperature of the heating element. Finally, safety considerations, including insulation, sensor accuracy, and user interface constraints are incorporated to make the jacket practical and secure for everyday use.

A 1.5 meter nichrome heating wire was determined to provide adequate heat output. Thermal testing was conducted on bare, insulated, and integrated setups to understand heat distribution. A custom power stage using a synchronous buck converter was designed and implemented. An Arduino development board, along with a display module and a suitable temperature sensor interface, controls and regulates the power stage. A graphical user interface allows the user to view and set the desired temperature. The jacket uses a cotton interfacing layer to distribute heat and shield users from direct contact with heating elements.

The prototype fell short of maintaining target temperatures with moderate accuracy and stability. Testing showed the temperature being in $\pm 5°C$ of desired user input of $45°C$ after around 10 minutes. Although limitations exist in battery life and uniformity of heat distribution, the project provides a viable foundation for future development and refinement of electrically heated clothing.

Keywords: Electrically heated clothing, Temperature control, Synchronous buck, Li-Po battery, Thermal jacket, Nichrome heating wire,

# Sammanfattning

Detta kandidatarbete undersöker design och implementering av en temperaturreglerad prototyp för en elektriskt uppvärmd jacka. Värme genereras i en nikromtråd då den belastas med effekt från ett litium-polymerbatteri. Effektleveransen hanteras genom en designad synkron buck-omvandlare. Ett proportionell-integrerande reglersystem har implementerats för att reglera utspänningen och stabilisera temperaturen i värmeelementet. Säkerhetsaspekter såsom isolering, sensorers noggrannhet och begränsningar i användargränssnittet har också tagits i beaktning för att göra jackan praktisk och säker för vardagligt bruk.

En 1,5 meter lång nikromtråd valdes som värmeelement då den gav tillräcklig värmeeffekt. Termiska tester genomfördes på rena, isolerade och integrerade uppsättningar för att analysera värmefördelningen. Ett specialdesignat kraftsteg med en synkron buck-omvandlare utvecklades och implementerades. En Arduino mikrokontroller, tillsammans med skärm och lämpligt gränssnitt mot temperatursensor, styr och reglerar kraftsteget. Ett grafiskt användargränssnitt gör det möjligt för användaren att se och ställa in önskad temperatur. Jackan är utrustad med ett fodrande lager av bomull som hjälper till att fördela värmen och skydda användaren från direktkontakt med värmeelementen. Säkerhetsfunktioner såsom en nödbrytare och en värmetröskel har integrerats för att förhindra överhettning eller personskador.

Prototypen uppnådde inte de angivna värdena för temperatur med godtagbar noggrannhet och stabilitet. Tester reslutera i tempraturer på $\pm 5°C$ på den bestämda tempraturen $45°C$ efter 10 minuter. Trots vissa begränsningar i batteritid och värmefördelning utgör projektet en god grund för vidareutveckling och förfining av elektriskt uppvärmda kläder.

# Acknowledgements

We would like to express our sincere gratitude to our supervisor, Vaishnavi Ravi at Chalmers University of Technology, for her valuable guidance and support throughout our Bachelor's thesis—both in the development of the jacket and in the writing of this report.

We also want to thank the CASE labs for assisting us in finding and using

Edvin Hansson, Moa Johnsson, Marcus Koponen Edvardsson
Alfred Lindell, Caroline Pohjanvuori, Felix Sjöstedt
Gothenburg, May 2025

# List of Acronyms

Below is the list of acronyms used throughout this thesis presented in alphabetical order:

| | |
|---|---|
| CCM | Continuous Conduction Mode |
| FOTD | First Order Time Delay |
| IC | Internal Circuit |
| I2C | Inter-Integrated Circuit |
| Li-Po | Lithium Polymer |
| MOSFET | Metal Oxide Semiconductor Field Effect Transistor |
| PCM | Phase Changing Material |
| PI | Proportional–Integral controller |
| PID | Proportional–Integral–Derivative controller |
| PWM | Pulse Width Modulation |

# Nomenclature

Below is the nomenclature of variables used throughout this thesis.

## Variables

| | |
|---|---|
| $V_c$ | Control voltage |
| $\Delta I$ | Current ripple |
| $D$ | Duty cycle |
| $f_c$ | Gain-crossover frequency |
| $V_d$ | Input voltage |
| $K_i$ | Integral gain |
| $T_i$ | Integral time constant |
| $f_B$ | Frequency bandwidth |
| $V_o$ | Output Voltage |
| $K_p$ | Proportional gain |
| $F_{sw}$ | Switching Frequency |
| $T_{sw}$ | Switching time period |
| $\Delta V$ | Voltage ripple |

# Contents

# 1

# Introduction

## 1.1 Background

Jackets are a must to keep warm in colder climates. Failure to keep warm can result in health problems and, in the worst case, serious injuries or conditions. Layered clothing can be used to control the temperature, however, it can be seen as bulky and hinder regular activities. This applies especially to people working in cold environments, differently abled, kids and sport-active people. A survey conducted in [1] amongst differently abled and caregivers reports that almost half struggled with finding outwear for their needs.

A solution to address this scenario is to use heated clothing. In [2], heated clothing was divided into four different categories. Solar-heated clothing, chemical-heated clothing, phase change material-heated clothing and electrically heated clothing. Electrically heated clothing is seen as the most viable alternative if there is interest in the user being able to control the temperature. Furthermore, electricity can be switched on and off by the user or the control system.

Electrically heated jackets are already available on the market, but they struggle with a few limitations [3]. Fundamentally, having preconditioned heating modes which lead to pre-defined working temperatures. These lack automatic temperature control and demand labour to keep the modes in check.

This project will explore and create a prototype of an electrically heated jacket with an automatic temperature-controlled system.

## 1.2 Aim

The project aims to develop a prototype of an electrically heated jacket with automatic temperature control.

The desired prototype should include the following:

- An appropriate heating element which is powered from a rechargeable battery.
- DC-DC converter stage, controlled by suitable controller to regulate the heat produced in the heating element.
- A user interface with a display unit displaying the current temperature as well as the desired temperature for added user controllability.
- Temperature sensors mounted suitably on the jacket to detect and control the heat produced, thereby achieving the desired temperature.

The prototype will also aim to implement easy detachment and reconnection of electronics, to support washing, daily wear and eventual reparations.

## 1.3 Scope

This project focuses on the development of an automatic temperature control system. Thus, the fabric and aesthetic of the jacket will not be considered. The jacket will be bought and the only qualities of importance are durability and strength. The environmental impact of the materials and jacket production will not be considered. Since this is only a prototype and not intended for mass production, its impact is deemed negligible.

Complex machine learning is another aspect that could be explored further, but not in this project. It could, for instance, be used to learn user behaviour, thus creating a more efficient heating pattern and even being able to predict the user input. This would in turn result in a better user experience and further increase the energy efficiency. For simplicity's sake as well as time limitation, a more arbitrary system with temperature limits will be implemented.

Mobile app connectivity is another feature of interest. However, it is beyond the scope of this project. Considering the time and resource limitation, an user interface with a display unit and physical buttons will be employed to set and monitor the temperature.

## 1.4 Previous work

A temperature-controlled jacket designed to both cool down and heat up the user has been made using Peltier modules [4]. When a current is passed through a Peltier module one side heats up while the other cools down. The study used multiple Peltier modules in the jacket, where the input from a temperature sensor was compared to the desired temperature, set by the wearer on an LCD screen. With this information, the central processing unit would either enable the modules with the cooling side towards the user, or the heating side.

Flexible printed heaters designed to be used in clothing have been tested for washability [5]. The heaters were pinned between pieces of fabric and washed in a washing bag. Initially, the heaters consumed 2.1 A at 5 V, and after 20 washes, both had decreased slightly. Thermal images also revealed that there was minimal breakdown of the electrical connectors on the heaters.

Another prior experiment is the introduction of Phase Changing Materials (PCMs) in clothing [6]. A PCM is a substance that transitions between solid and liquid states and releases or absorbs heat in the transitioning process. This enables an article of clothing, not only able to heat the user, but also cool the user down.

Another commonly used method when it comes to producing heat is a chemical heating system. A chemical heating system is more commonly used to alternate and give an option to electrical heating, for instance, if access to electricity is limited or to support in emergencies [7]. Despite their ease of access and reliability, use cases outside of single-time use are scarce because of their baseline properties. The chemical heating system generates heat by chemical reactions, and such reactions are hard to repeat.

A rather recent implementation is that of graphene in electrically heated jackets [8]. It has been shown to increase the temperature of the clothing while also maintaining comfort at lower temperatures. However, it seems that higher levels of heating can cause uneven distribution of the heat, thus affecting the comfort.

The research of heated jackets has come quite far, with researchers recently implementing a user interface that lets the wearer control the temperatures of specific body parts [9]. This was mostly done to achieve better human performance, but also to reduce energy expenditure. This offers what is called a personal microclimate, and its intended use is everyday clothing.

# 2

# Theory

In this chapter, the theoretical aspects of the temperature-controlled jacket are outlined. A general system-level block diagram of the jacket is presented in Figure 2.1. The theoretical aspects involved in the selection of various subsystems are presented as follows.

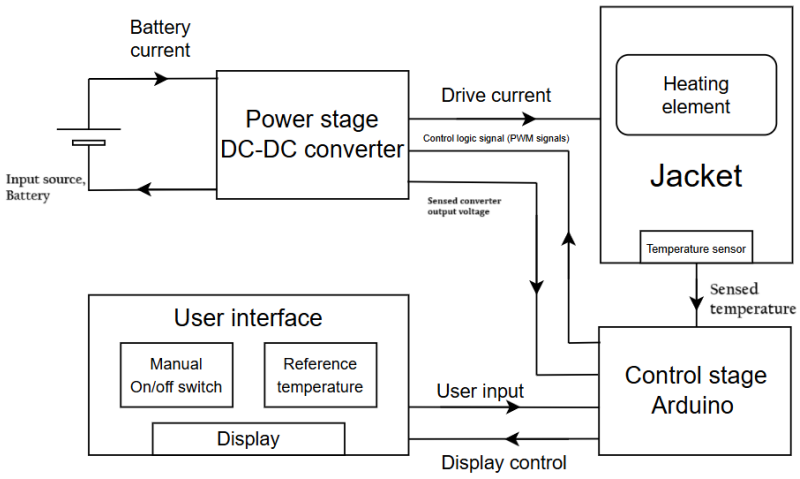


**Figure 2.1:** The system level diagram of the assembled system

## 2.1 Heating elements

There are different methods that can be used to electrically heat garments. A few of those are discussed below.

### 2.1.1 Metal wire

Metal wire heating elements are composed of a metal wire encased in an insulation material [10]. These heating elements operate on the principle of Joule heating, where heat is generated when a current flows through the wire. For electrically heated garments, materials such as nichrome, an alloy made of nickel and chromium, aluminium-chrome, and tungsten are suitable to use, because of their efficient heat generation [11] [12].

The main purpose of the insulation material is to prevent heat loss [13]. By retaining the heat in the system, the effectiveness of the heating elements is maximised. Another important role of insulation is to protect the metal wire from coming in contact with the neighbouring conductive material, components and the user. This layer also acts as a shield against moisture and physical damage. Some commonly used insulations are silicone rubber and fibreglass sleeves. While silicone rubber is a softer and more flexible material, fibreglass can withstand higher temperatures, and it is more robust [14][15].

#### 2.1.1.1 Heat transfer with metal wires

It is ideal to place the wires in a wave pattern to increase the heating elements' area and maximise heat transfer [16]. According to Newton's law of cooling,

$$\dot{Q} = \oint_A h\Delta T(t)dA \tag{2.1}$$

where, $\dot{Q}$ is the rate of heat transfer out of the body, $h$ is the heat transfer coefficient, $A$ is the heat transfer surface area and $\Delta T(t)$ is the time dependent temperature difference between the environment and object. The larger the area, the better the heat transfer [17]. The wires alone have a limited area, but if the wires are laid out in a wave format, they can be aggregated into a heat transfer surface area. Such a pattern can be seen in Figure 2.2.

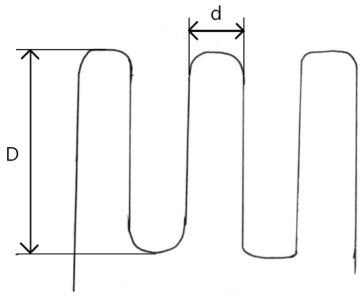


**Figure 2.2:** A wave format wire where $D > d$

This avoids greater heat spots due to the uneven heat distribution of metal wires.

The foldability of wires is limited, easily bending and deforming on the long side D, see Figure 2.2 [18]. The short horizontal wire lines d need more applied force to bend [19]. Thus, the long side D must be oriented to the side that bends the least. Figure 2.3 illustrates the impact of bend stress on the wire.

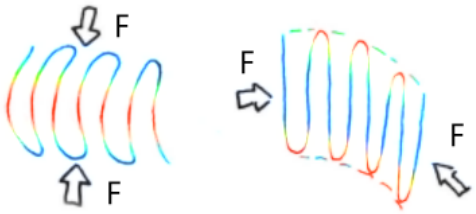


**Figure 2.3:** a wave format wire's bend stress depending on a horizontal or longitudinal force F

### 2.1.2 Carbon fiber

Carbon fibre heating elements, similar to metal wire heating elements, also operate based on Joule heating [10]. This process is efficient because of the high electrical conductivity and thermal stability of carbon material, making it a strong choice for consistent and controlled heating applications.

Carbon fibre has been integrated into wearable technology, particularly in clothing designed for cold environments, such as gloves and knee pads [20]. They have features such as being lightweight, having high flexibility and breathability, which is critical for the heating elements used in clothing [21].

However, there are some challenges in the production and integration of carbon fibre heating elements. The process of embedding these fibres into textiles can be complex and time-consuming, which may lead to higher production costs [22]. In addition to this, working with carbon fibre can release respirable fibres into the air, which could pose health risks if inhaled [23].

### 2.1.3 Silicone heating pad

A silicone heating pad is a flexible metal heating element [14][24]. It uses both resistance wire and etched foil embedded in silicone rubber. This combination ensures a precise and uniform heat distribution. The silicone rubber provides added durability, mechanical flexibility, and high thermal resistance, making it ideal for applications such as heated jackets. However, silicone heating pads are limited in customisation since they come in predefined sizes, and resizing them is not possible. This can be a limiting factor when trying to tailor the pad to specific needs. The price can also be a concern, especially with the larger sizes, as they can be quite expensive.

## 2.2 Lithium polymer battery

A Lithium Polymer (Li-Po) battery is a type of rechargeable battery, commonly used in portable applications because of its lightweight, flexibility and high energy density [25]. Li-Po batteries lack metal, which gives them these properties [25]. Most Li-Po batteries consist of a graphite anode, a cathode made of metal oxides, and an electrolyte consisting of a polymer along with a lithium-ion-conductive liquid electrolyte, which forms a gel configuration [26][27]. There is typically a separator that prevents the anode and cathode from coming in contact.

The operation of Li-Po batteries involves the movement of lithium ions between the anode and cathode[25]. During the charging process, lithium ions move from the cathode to the anode. When discharging, the ions move from the anode to the cathode instead, generating electrical energy. Li-Po batteries tend to have good cycle life because of their flexible construction, allowing the electrodes to expand and contract during the cycle.

Relevant safety measures need to be considered when using the LiPo batteries, especially for wearable applications. Different injury thresholds on the human body based on the subjected current are described in [28].

## 2.3 DC-DC converter

DC-DC converters are generally employed in battery-powered applications to regulate and control the power delivered from the battery to the load. A buck converter is a step-down DC-DC converter where the average output voltage $V_o$ is less than the input voltage $V_d$ [29]. The circuit diagram of a buck converter with a resistive load is shown in Figure 2.4.

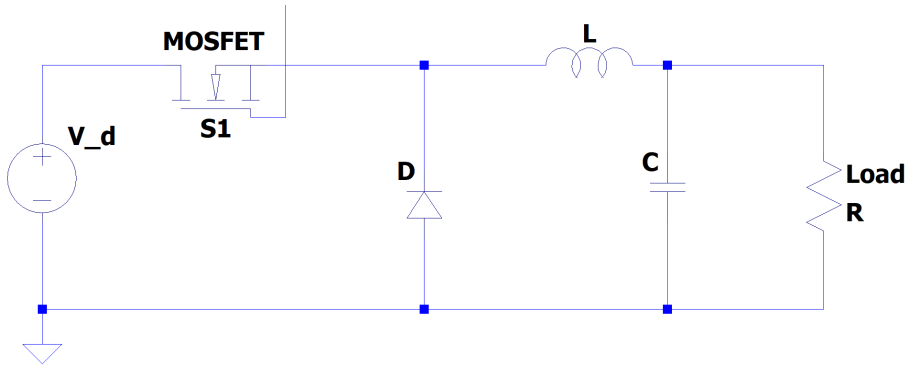


**Figure 2.4:** Circuit diagram of a buck converter

The circuit works by controlling the MOSFET switch ON and OFF at a switching frequency in the range of $50\,kHz$ to $500\,kHz$ [29]. During $T_{on}$, the MOSFET conducts and the current flows from the battery with input voltage $V_d$ through the MOSFET, inductor, capacitor and the load. When the MOSFET is off, then the current flows through the diode, inductor, capacitor and load. Thus, the energy

from the battery is stored in the energy storage elements, the inductor and the capacitor, and delivered to the load. The duty ratio ($D$) is the percentage of time that the MOSFET is ON; mathematically, this is given by,

$$D = \frac{t_{on}}{T_{sw}} \tag{2.2}$$

where $T_{sw} = 1/F_{sw}$ and $F_{sw}$ corresponds to the switching frequency at which the MOSFET operates [29]. The output voltage $V_o$ over the load can be calculated from the input voltage $V_d$ and duty ratio as

$$V_o = \frac{1}{T_{sw}} \int_0^{T_{sw}} V_L(t)dt = \frac{1}{T_{sw}} (\int_0^{t_{on}} V_d dt + \int_{t_{on}}^{T_{sw}} 0dt) = \frac{t_{on}}{T_{sw}} V_d = DV_d \tag{2.3}$$

$V_o$ can be varied with constant $V_d$ by changing the duty ratio D. The duty ratio is typically in the range $10 - 90\%$. A low-pass filter, consisting of a capacitor and an inductor, on the output side of the buck converter aids in reducing the output voltage fluctuations and filters out switching frequency noise [29]. Without the low-pass filter, the output voltage would be a rectangular pulse, alternating between the amplitude $V_d$ and $0\,V$. By selecting the corner frequency $f_c$ to be much lower than the switching frequency, the high-frequency switching noise is filtered, and the average output voltage is obtained at the load. The corner frequency $f_c$ can be calculated from

$$f_c = \frac{1}{2\pi\sqrt{LC}} \tag{2.4}$$

A synchronous buck converter is preferred over a conventional buck converter, because of better efficiency, reduced loss and better battery utilisation. The circuit diagram of synchronous buck is presented in Figure 2.5.

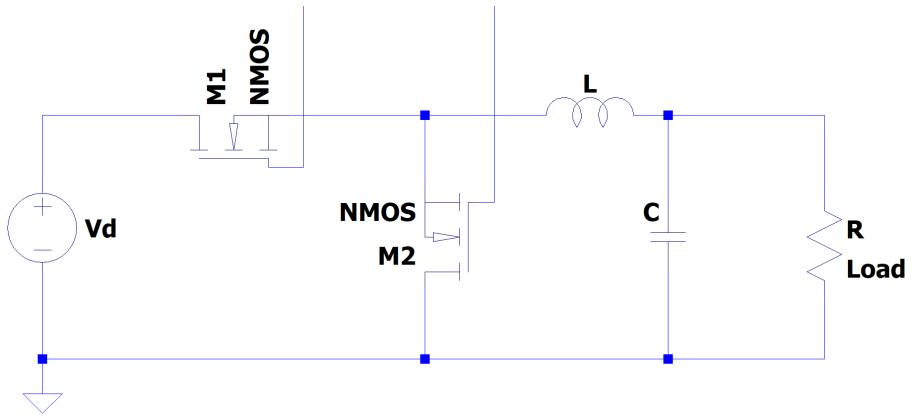


**Figure 2.5:** Circuit diagram of a synchronous buck converter

In a synchronous buck converter, the low-side diode is replaced by an active MOSFET, ensuring a lower voltage drop compared to the diode [29]. The inductance and capacitance of the buck converter are designed based on the allowable current ($\Delta I$) and voltage ripple ($\Delta V_o$), respectively. D is the duty ratio, $V_d$ is the input voltage, and $V_o$ is the output voltage. $\Delta I_L$ is the peak-to-peak current ripple (difference

between maximum and minimum inductor currents) passing through the inductor and should generally be within $20 - 30\%$ of the current. $\Delta V_o$ is the peak-to-peak output voltage ripple and should generally be less than 1%. The switching frequency $f_{sw}$ is usually in the range of $50\,kHz$ to $500\,kHz$ [30]. The inductance value can be calculated with

$$L = \frac{(V_d - V_o) \cdot D}{\Delta I_L \cdot f_{sw}} = \frac{V_d D(1-D)}{\Delta I_L \cdot f_{sw}} \tag{2.5}$$

and the capacitance $C$ is calculated with

$$C = \frac{\Delta I_L}{8 \cdot \Delta V_o \cdot f_{sw}}. \tag{2.6}$$

To drive the MOSFETs and control the output voltage, Pulse Width Modulation (PWM) needs to be implemented [29]. A PWM signal is a rectangular wave with the ability to vary the duty cycle. Generally, a suitable controller is used to output a variable PWM signal[31]. A MOSFET driver IC can be used to drive the gate of the high-side MOSFET in the synchronous buck converter over $V_d$ and drive the low-side MOSFET with the complementary signal.

## 2.4 Sensing and Control system

An appropriate temperature sensor is critical in designing a temperature-controlled jacket. The temperature sensor provides an analogue signal or voltage to the master, corresponding to the detected temperature. A traditional sensor IC sends a certain voltage to the analogue pin, corresponding to the temperature measured [32]. An IC sensor can also provide a digital output with certain bits, equivalent to a voltage and can be communicated via I2C (Inter Integrated Circuit) or SPI (Serial Peripheral Interface) protocols.

A suitable controller that takes input from multiple sensors and generates desired PWM signals to control the MOSFETs is generally employed together with buck converters. The controller, based on the input sensed signals and implemented control logic, generates desired PWM signals. The simplest control system that could be implemented with a buck converter is a Proportional Integral (PI) controller [29].

For modelling the delay of a temperature sensor, a First Order Time Delay (FOTD) is stated in the laplace domain as

$$P(s) = \frac{K_{gain}}{1 + sT} e^{-sL}, \tag{2.7}$$

where, $K_{gain}$ is the gain constant that scales the output, T is the time-constant, and L is the dead time before changes in the system can be seen [33]. The model takes into account the sensor's response time before changes can be seen of the generated values. FOTD is commonly found in the process industry, where there are inherent delays between inputs and outputs.

# 3

# Method

This chapter discusses the method followed in the design, selection, and implementation of the various components of the temperature controlled thermal jacket.

## 3.1 Selecting battery

When selecting the battery, the most important parameters were the weight and nominal voltage and battery capacity. The battery needed to be lightweight and safe to be implemented in the wearable application. The Li-Po battery SUNPADOW SW256415 was chosen. Its specification values can be seen in Table 3.1. The selection of a 5400 $mAh$ capacity for the battery is discussed in a later section of 3.3.5.

**Table 3.1:** The battery specifications and capacity

| Nominal voltage | Capacity | Weight |
|---|---|---|
| 11.1 $V$ | 5400 $mAh$ | 0.327 $kg$ |

Some aspects to note when using the electrical source in a wearable jacket are: if there is body contact with the circuit through dry skin, a barely noticeable current will flow through the body [28]. If there is body contact with the circuit through wet skin, there will be a slight tingling shock. Meanwhile, if the circuit is in contact with an open wound or inside a human body, it will result in a painful shock.

## 3.2 Selecting heating element

When selecting the heating element, two solutions were considered. First, a silicone heating pad was considered. However, silicone heating pads were expensive and not within the budget, and thus, they were deemed an unviable option. Alternatively, a more cost-effective solution was to employ heating wires, where the thickness of the wire and resistance per meter were important. A nichrome wire with a diameter of $0.711\,mm$ and resistance of $2.71\,\Omega/m$ was selected.

The length of the wire was the most deciding factor of the resistance, which needed to be balanced to reach the needed power output. Since the battery has an output voltage of $V_o = 11.1\,V$ and the maximum duty cycle the buck operates with is 95%, the wire could be powered with at most $10.5\,V$. It was decided to use a current of $2 - 3\,A$ because it corresponds with the typical wattage of a heated jacket[34]. The length of the wire can then be calculated as

$$l = \frac{V}{I \cdot R}[m] \tag{3.1}$$

where, $l$ is the length of the wire, $V$ is the voltage over the wires, $I$ is the current, and $R$ is the resistance per meter. The wire should be between 1.2 and 1.8 meters to get an appropriate power output. The length chosen was $1.5\,m$ as a middle ground.

Tests were performed on a 1.5 $m$ cable to determine heat output from different input voltages. There were four cases: a naked cable, a shielded cable, the shielded cable sewn into the interfacing pad, and the interfacing sewn into the jacket. The use of shielding, an interfacing pad and the implementation into the jacket is explained in Section 3.4. The temperature was measured at three points on the cable after 60 seconds with a Fluke IR thermometer 62 max+. This thermometer has a measurement error of $\pm 1\,°C$[35]. Since the measurement area was so thin, the wire had a diameter of 0.711 $mm$, this measurement error is in practice higher. The temperature was measured by aiming the laser directly at the heating wire. On the jacket, the wire was not visible. Instead, three temperatures were noted that were high enough to be presumed to be close to the heating wire. This also increases the measurement error. The results of each test can be seen in Figure 3.1.

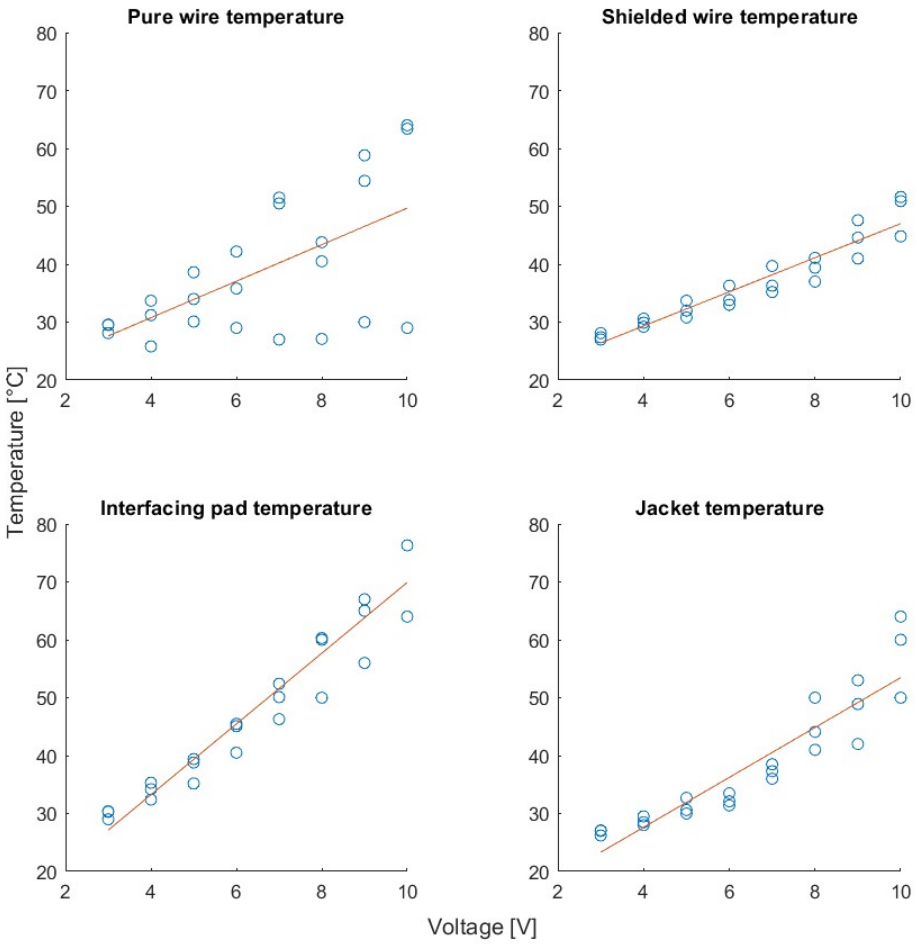


**Figure 3.1:** Temperatures of the heating pads layers with different voltages

Since temperature sensors would be mounted on the interfacing pads, an analytical function was derived from the result of the interfacing pad. The temperature increase

was approximated as linear and the resulting function can be described by

$$T = 6.1 \cdot V + 8.8\,[^{\circ}C] \tag{3.2}$$

where, $T$ is the temperature and $V$ is the voltage over the wires. The temperature at $10\,V$ according to this function is $69.8\,^{\circ}C$, higher than the maximum temperature. This is not a problem for the control system, but an additional emergency switch was needed to override the control and hardware to stop the system. If the temperature rises too high, this switch can be used to break the circuit. All tests were carried out in room temperature. Infrared images of heat distribution in the jacket were taken with the help of the thermal camera. However, since the camera's measurement errors were large in comparison with the fluke thermometer, the results from fluke thermometer were taken for analytical formulation of relation between voltage and temperature. These figures are presented in Chapter 4.2.

## 3.3 Power stage

The power stage consisted of a buck converter, which was connected to the battery. The power stage is then connected to the heating element and the control stage. To drive the power stage, an Arduino UNO capable of producing a PWM, among other functions presented in section 3.5.2, was chosen as a controller[36]. And the output voltage of the power stage drives the heating element. The design of the various components of the buck converter was as follows.

### 3.3.1 Inductance selection

The inductance was calculated by following (2.5). The buck converter's switching frequency was first assumed to be $100\,kHz$. The current ripple was ensured to be within 30% of $I_{out}$. To ensure a balance between the size of the inductor and the allowable ripple, the value of the inductance was calculated in mid-operational duty, which is 50%. $\Delta I = 0.3 \cdot \frac{5.5}{4.2} = 0.392\,A$. These values were inserted into (2.5),

$$L = \frac{11.1 \cdot 0.5(1 - 0.5)}{0.392 \cdot 100\,kHz} = 70.8\,\mu H$$

where the value of inductance was found to be $70\,\mu H$. An inductor of $68\,\mu H$ (part No: 7447033) from Wurth Electronic was selected for implementation.

### 3.3.2 Capacitor selection

The output voltage ripple $\Delta V_o$ was chosen to be at most 1% of $V_o$. With these values inserted into (2.6)

$$C = \frac{0.392}{8 \cdot 0.111 \cdot 100\,kHz} = 4.41\,\mu F$$

a capacitance of $4.41\,\mu F$ was calculated. A capacitor model 711-2046 from RS components with a slightly larger capacitance of $10\,\mu F$ was chosen.

### 3.3.3 MOSFET selection

N-channel MOSFETs are preferred for implementation, because of their better switching characteristics compared to P-channel MOSFETs [37]. In the synchronous buck converter, two N-channel MOSFETs were used as the high-side and low-side switches. MOSFETs of model IRLZ44NPBF were capable of handling the voltage and current in the converter and were selected for implementation [38].

### 3.3.4 Driver IC selection

To drive the N-channel MOSFETs with a voltage at the gate greater than the source, based on the control PWM signals from Arduino, an appropriate driver IC was required. IR2184 IC includes bootstrap circuitry and is capable of driving the top and bottom MOSFETs of a synchronous buck [39]. The driver IC's pins had the layout as in Figure 3.2. Suitable bootstrap capacitor and diode were connected to the pins of the IC according to the values specified in the datasheet[39].

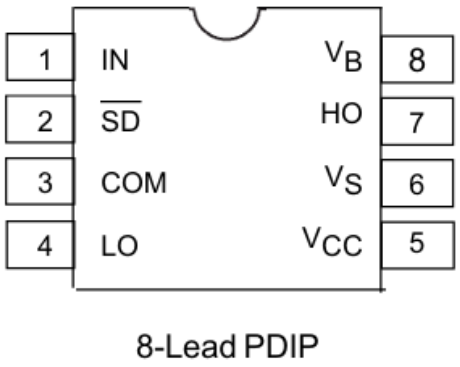


**Figure 3.2:** pins on the driver IC

### 3.3.5 Dimensioning of the battery

The maximum current required to drive the heating element $4.2\,\Omega$ to $60\,°C$ with $10\,V$ was $2.3\,A$. Figure 3.1 showed that a voltage of around $4\,V$ was required to ensure a constant temperature of around $30\,°C$. This corresponds to a current of around $0.95\,A$. To continuously discharge for 6 hours, a battery of around $5.7\,Ah$ was required. However, to maintain the temperature, a lower current could be sufficient. Thus, a Li-Po battery with a capacity of $5400\,mAh$ was selected.

### 3.3.6 Simulation of buck converter

A simulation of the buck converter was performed in LT-Spice with SPICE models of the chosen components. The simulation model can be seen in Figure 3.3. The load was set to $4.2\,\Omega$ corresponding to a $1.5\,m$ heating wire. To drive the driver IC, a sub-circuit was connected as per the data sheet's instruction[39]. The resulting voltage output from the circuit, along with the gate source voltage of the MOSFET, and the current flowing through the inductor, is presented in Figure 3.4.

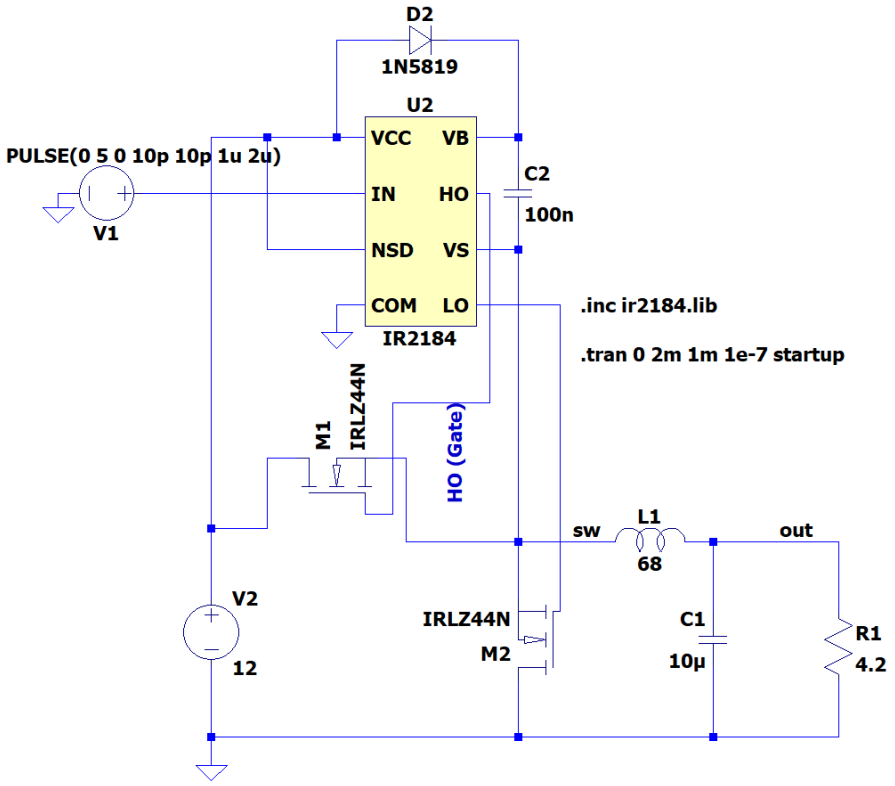


**Figure 3.3:** The circuit diagram of the buck with existing components

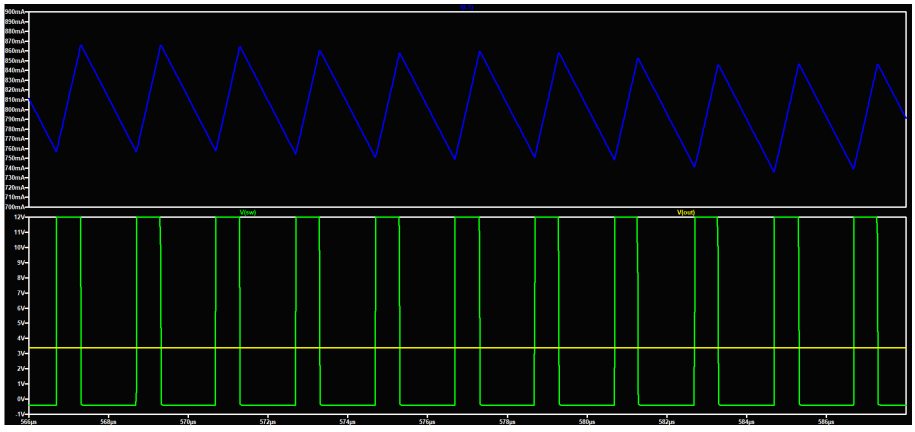

**Figure 3.4:** The result of simulating the buck with a 33% duty cycle. The green V(sw) is the voltage from drain pin of the MOSFET, the yellow V(out) is the voltage level over the load or heating element, and the blue I(L1) is the current going through the 68 $\mu H$ inductor.

### 3.3.7 Buck converter implementation

The components were soldered onto a general-purpose PCB as seen in Figure 3.5. The resulting circuit had two notable additions compared to the simulation. The first is a gate resistance, which was chosen to be 100 Ω, between the output of the driver IC and the gate of the MOSFETs. Secondly, the Arduino needed to read

the output voltage, which was solved by implementing a voltage divider. A PI controller to regulate the output voltage was designed as discussed in section 3.5.4 and is designed in the Arduino IDE code to generate the desired PWM. Upon testing with the physical circuit, it was found that a switching frequency of $50\,kHz$ worked better with the driver IC and MOSFETs. The already dimensioned inductor and capacitor values ran smoothly with this switching frequency, and therefore were not changed. An encasing for the buck converter circuit board was designed and then 3D printed. The resulting buck converter is presented in Figure 3.6.

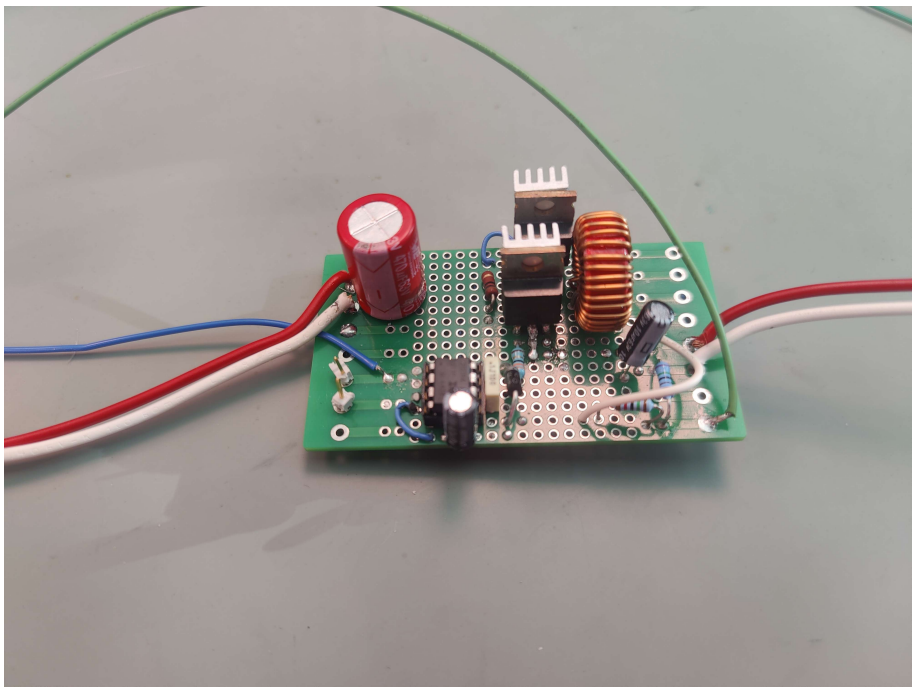

**Figure 3.5:** The soldered PCB board of the buck converter

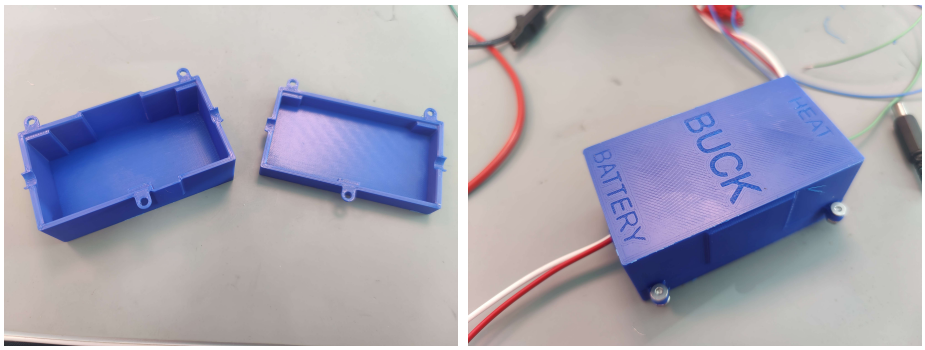


**Figure 3.6:** The encasing of the buck converter

## 3.4 Fabric and jacket interfacing considerations

To ensure better heat distribution and protect the user from direct contact with the fibreglass shielding, which can cause skin irritation, interfacing between the

heating element and the user was required [40]. A non-woven cotton fabric was chosen, a standard for many similar products on the market [41]. With this, the wires were sandwiched between interfacing pads. According to the product ironing specifications, the interfacing can be ironed on medium heat, around 180 °$C$ [42].

### 3.4.1 Jacket selection

A robust working jacket with thinner interfacing and a firm outside shell was chosen. According to the jacket's ironing specifications, it can withstand around 120 °$C$, corresponding to the lowest temperature setting on an iron [42]. The wires were arranged as discussed in Section 2. The pads were placed between the jacket's interfacing and inner lining fabric. The User Interface (UI) and buck converter were placed in the left inner pocket, while the battery was placed in a pocket on the back. The battery placements were selected to retain balance in the jacket. The jacket layout can be seen in Figure 3.7.

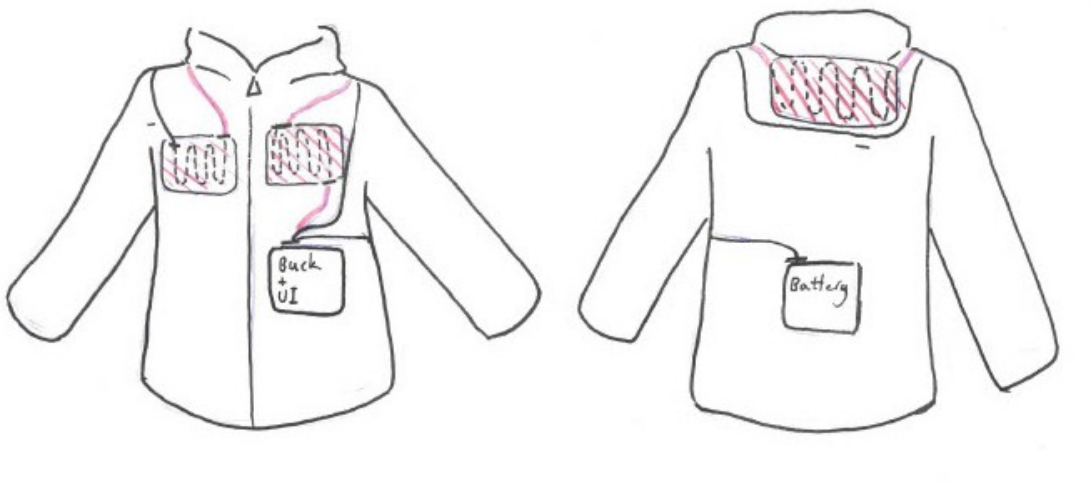


**Figure 3.7:** Jacket circuit and component layout

## 3.5 Sensing and control

### 3.5.1 User interface

The user interface has two main functions: to display the set temperature and to give the user the opportunity to change the temperature. The layout of the interface is shown in Figure 3.8.

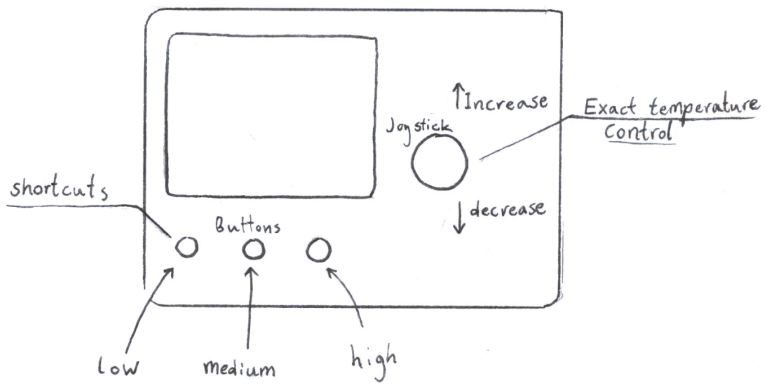


**Figure 3.8:** User interface with display and control buttons

The display component selected for implementation is Adafruit's 1.8" TFT Display Breakout and Shield. The buttons include three smaller spring buttons and one joystick. By moving the joysticks up or down, the exact temperature could be controlled, and the smaller buttons were shortcuts to low, medium and high temperature settings. The control cannot go below $30\,°C$ or above $58\,°C$.

### 3.5.2 Microcontroller

The controller had to be capable of reading temperature sensors, sensing the output voltage and producing PWM signals with a variable duty cycle. It also needed to be able to function with the UI. An Arduino UNO rev 4 model ABX00087 was chosen [36].

### 3.5.3 Sensors

#### Temperature

A few different temperature sensors were initially considered for the control system. It was decided that a sensor IC would be used because of their low cost, size, accuracy, and positioning required to be beside the heat source. The first sensor tested, the LM35, had a thermal response time of approximately 1 minute to reach 63% of the final value [32]. In contrast, the chosen sensor ChipCap 2-SIP had a response time of 5 seconds to reach 63% of the final value[43]. This made it more appropriate for the intended control system.

Originally, the plan was to have two or three sensors, one placed by the back heating element and the other two on the front heating elements. This was in order to ensure a balanced average temperature regulation. However, the I2C protocol did not support controlling multiple sensors individually because multiple sensors needed to refer to the same address, which made multiple separate data buses impossible. As a result, only one temperature sensor could be used, which was placed beside the back heating element.

### Voltage

To measure the output voltage from the buck converter, a simple voltage divider was implemented by placing two resistors in series between the output voltage and ground, as shown in Figure 3.9. The voltage at the node between the resistors was scaled down, and a sensing wire was connected at the scaling node to one of the Arduino ADC channels. This configuration allowed the Arduino to safely read the scaled down voltage, ensuring it remained within the 0–5 V input range and preventing any risk of exceeding the Arduino voltage limit. Resistors $R_1 = 15\,\text{k}\Omega$ and $R_2 = 7.5\,\text{k}\Omega$ were used for scaling the output voltage.

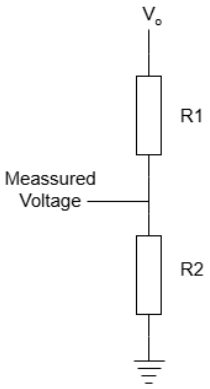


**Figure 3.9:** Circuit diagram of the voltage divider

### 3.5.4 Control system

A cascaded-loop is shown in Figure 3.10: the outer temperature controller computes a voltage reference for the inner buck-converter voltage controller, which in turn drives the power stage. This was the model the control system is based on.

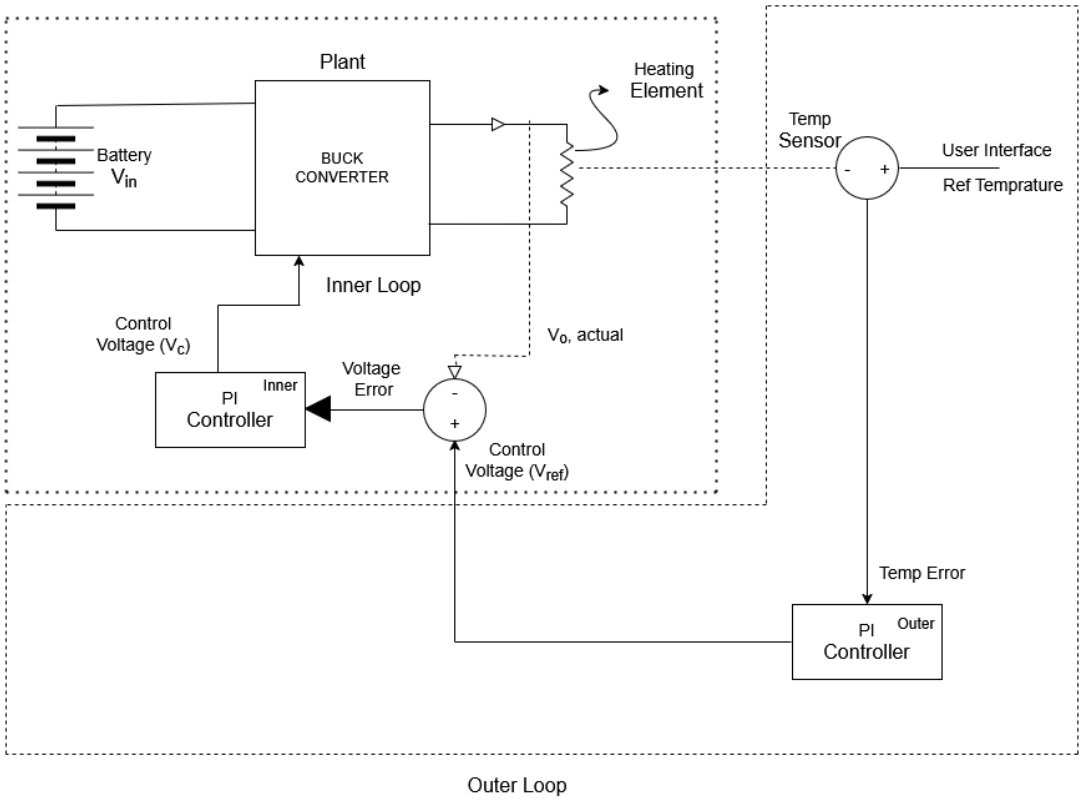


**Figure 3.10:** Inner Loop and Outer Loop of the system

#### 3.5.4.1 Inner-Loop Control

The inner loop regulates the voltage over the buck converter. The input to the inner loop is the reference control voltage. This reference was from the outer temperature loop and the output terminals sensed voltage from the buck converter. The inner loop PI controller was designed from the small signal transfer function of the buck converter. The model corresponding to Continuous Conduction Mode (CCM) was used [29]. The buck converters small signal model $G_{vd(s)}$ is given by

$$G_{vd}(s) = \frac{V_{in}}{LCs^2 + \frac{L}{R}s + 1} \tag{3.3}$$

where L, C and R were given by the components in the buck converter.

The voltage divider gain, H(s), was also part of the controller. The voltage was downscaled to be read from the Arduino. The plant process is therefore defined as

$$G_{plant}(s) = H(s)G_{vd}(s) = \frac{1}{3}\frac{V_{in}}{LCs^2 + \frac{L}{R}s + 1} \tag{3.4}$$

where, H(s)=1/3 was the voltage divider gain from output voltage to the sensor voltage.

Inserting the values into the transfer function gives

$$G_{plant}(s) = \frac{3.7}{8 \cdot 10^{-10}s^2 + 1.968 \cdot 10^{-5}s + 1} \tag{3.5}$$

where the transfer function describes how small changes in the duty-cycle, D, lead to changes in the output. In the chosen implementation, the DC-DC converter will operate in the range of 20% to 95%.

Generally, the controller is designed for switching converters in a way that the gain crossover frequency is at 1/10 or less than the switching frequency, and the phase margin is greater than 45° and less than 60° [29]. A MATLAB code was written to compute the PI regulator values meeting the above constraints. The desired phase was set to 60° for stability reasons. The buck converter operates on a $50\,kHz$ and the desired bandwidth is kept at 1/10th of the switching frequency. Therefore, the cross-frequency was chosen to be $\omega_c = 2\pi \cdot 5 \cdot 10^3 = 31400$ rad/s.

The phase of the controller, $\angle F(j\omega_c)$, can be determined by calculating

$$\angle F(j\omega_c) = -180° + \varphi_m - \angle G(j\omega_c) \tag{3.6}$$

where $\angle G(j\omega_c)$ was the phase of the process at the selected cross frequency, and $\varphi_m$ was the phase margin. The PI regulator is usually represented as, $Kp + Ki/s$; which is rewritten as, $Kp(1 + 1/STi)$, because $Ki$ is equal to $Kp/Ti$. The values of $Kp$ and $Ki$ are determined to reach the overall system's desired bandwidth and phase margin. This can then be tuned to compute $Kp$ and $Ti$ by solving the standard magnitude and phase equations. The frequency of the system and the step response of the system is presented in Figure 3.11.

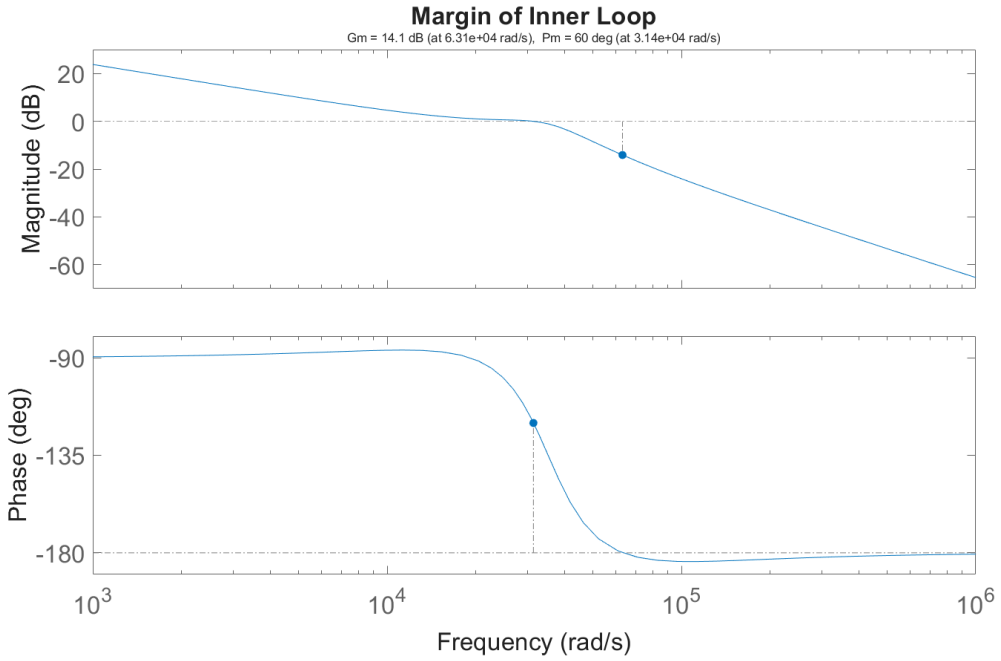


**(a)** Frequency response of the inner loop

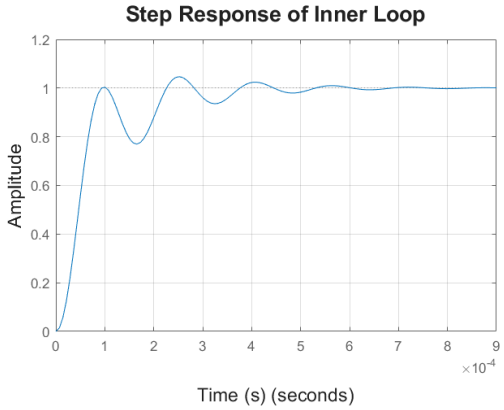


**(b)** Step response of the inner loop

**Figure 3.11:** (a) Open loop margin and (b) Inner loop step response of the system

#### 3.5.4.2 Outer-Loop Control

The outer loop performs the temperature control, taking the reference temperature input from the user and sensed actual temperature from the temperature sensor. The outer loop is modelled as a FOTD system as shown in

$$G_{\text{sens}}(s) = \frac{K_{gain}}{1+Ts}e^{-Ls}. \tag{3.7}$$

The PI controller for the outer loop is designed following lambda tuning [33]. The outer loop computes the required reference voltage and sends it to the inner voltage control loop.

#### 3.5.4.3 Discretization and Implementation

To implement the PI controller in Arduino, the Tustin method is used to convert continuous to discrete domain. Matlab was used, where the function C2D was called on the two PI-regulators described and formulated as

$$u[k] = u[k-1] + b_0 e[k] + b_1 e[k-1], \quad b_0 = kp + \frac{k_i T_s}{2}, \quad b_1 = -kp + \frac{k_i T_s}{2}, \tag{3.8}$$

where $k$ is the current sampled data and $k-1$ is from the previous sample. Suitable control limits and anti-wind-up is implemented in the code to avoid over accumulations in the integrator.

The update interval $T_s$ is the duty-cycle of the buck converter at $20\,\mu$s and $T_s$ for the outer loop is 0.1 s. Thus, the outer loop runs at a slower rate than the inner loop by a factor of $0.1/(20 \cdot 10^{-6}) = 5000$. This means the inner loop updates approximately 5000 times for every outer loop update, which is desirable for stable nested control.

Control limits are defined around the minimum and maximum duty cycle, D, of buck converter. Consequently set to be defined between $C_V$ from $0 - 10.5$. Clamping was used for anti wind-up in both regulators.

# 4

# Results and Discussion

This chapter discusses the results obtained from the tests carried out on the buck converter and the heating elements.

## 4.1 Background and Context

This section will provide clear context for the processes and results of the project.

### 4.1.1 Project Purpose

The project aimed to develop a prototype of an electrically heated jacket with automatic temperature control. The defined goals were:

- A functional Heating element
- Rechargeable battery
- DC-DC converter stage
- Control system for the heating element
- A sensor to keep track of the real temperature in the jacket
- User interface that lets a user set a desired temperature for the system
- A display to show the desired temperature and the real temperature
- Easily detachable components
- Washable
- Repairable
- Usable in daily wear

## 4.2 Summary of Key Results

The following sections present the results from the implemented prototype.

### 4.2.1 Buck Converter

The hardware results from the designed buck converter is presented in Figure 4.1. Initial tests were performed with a power supply set to 11.1 $V$. In Figure 4.1, the gate and drain (source) voltages are presented for 20% and 95% duty cycle. When the MOSFET conducts, the drain-source voltage is close to zero (with the condition drop of the MOSFET), and the current is carried by the MOSFET. In Figure 4.2, the Arduino control PWM is presented alongside the high-side MOSFET and the low-side MOSFET. The two MOSFETs gate signals are complementary, as seen, with the driver ensuring the intended operation of a synchronous buck. In Figure 4.3, output from the Arduino and the driver is presented, corresponding to maximum and minimum allowable duty used in the controller implementation. The duty percentages, which are an output voltage of around 2 $V$ and 10 $V$, respectively.

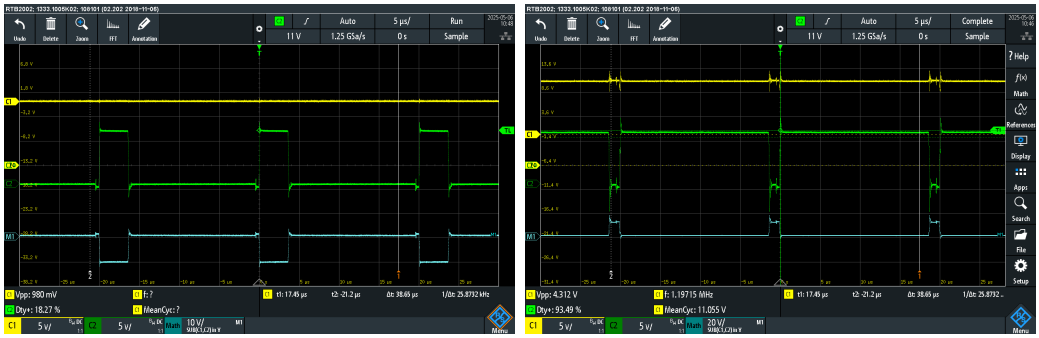

**Figure 4.1:** The yellow signal is the drain voltage of the high side MOSFET, at around 11 $V$. The green signal is the gate voltage of the high side MOSFET. The blue is the drain source voltage. The left image has a duty percentage of 20% and the right has a 95%

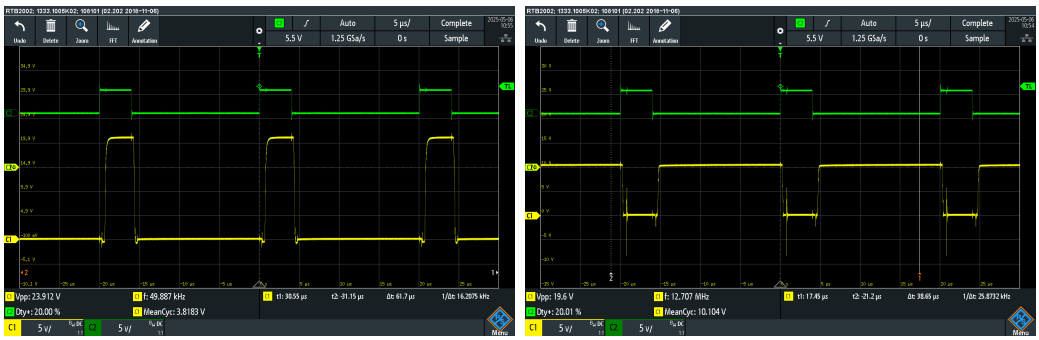

**Figure 4.2:** The green signal is a PWM sent from the Arduino with a duty percentage of 20% in both images. The yellow signal from the left image is the source of the high-side MOSFET, and the yellow signal from the right image is the source of the low-side MOSFET.

**Figure 4.3:** The green signal is a PWM sent from the Arduino with a duty percentage of 20% on the left image and a duty percentage of 95% on the right image. The yellow signals are the output voltage $V_o$ of the buck with respect to the duty cycles. The left output voltage is around $2\,V$ and the right output voltage is around $10\,V$

### 4.2.2 Heating element

The jacket through an infrared camera can be seen in Figure 4.4. The heat is spread out, but heat spots still appear.

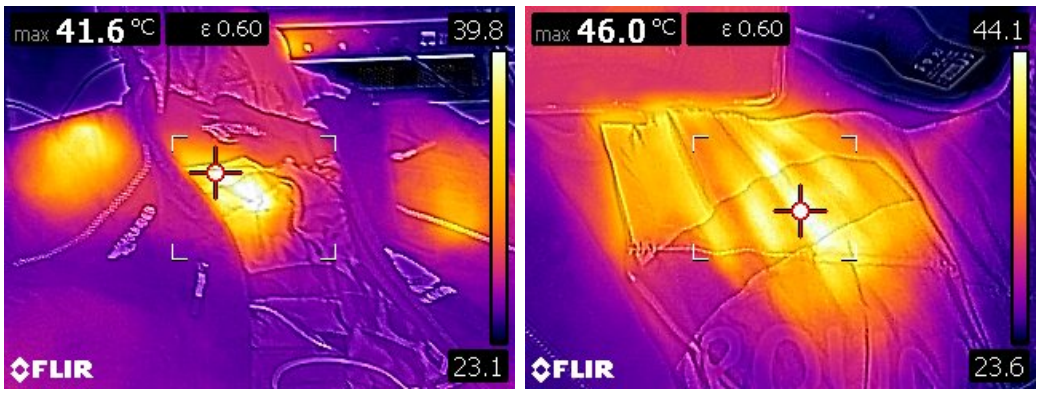


**Figure 4.4:** Jacket with a desired temperature of 45 degrees through a thermal camera, the left being all heat pads, the right a detailed look at the backs heat pattern.

### 4.2.3 User interface

The UI display and control are shown in Figure 4.5. The display shows the desired temperature. The buttons worked as described in Chapter 3. The Arduino and sensing cables are encased in a 3D printed case and a piece of acrylic to protect the screen.

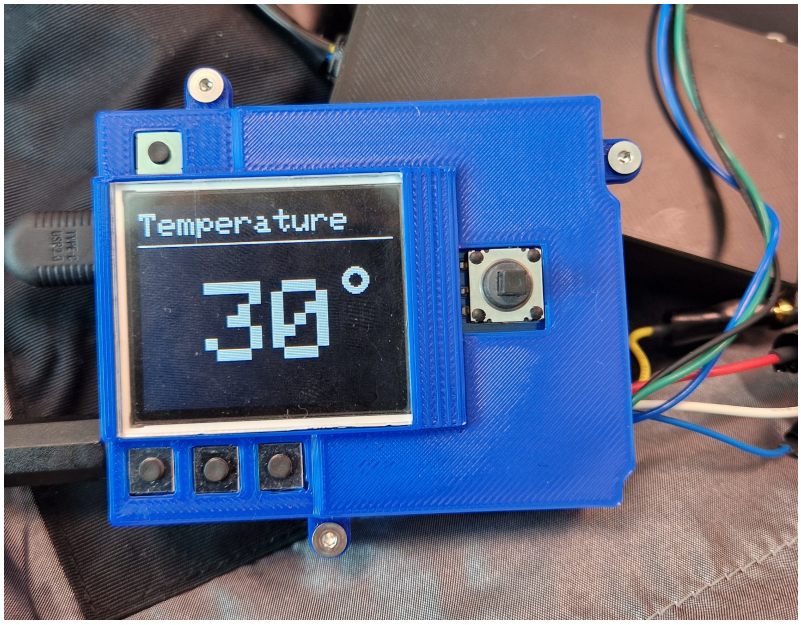


**Figure 4.5:** The display and design of the controller

### 4.2.4 Control System

In the Figure 4.6, the resulting signals from the controller are presented. The desired temperature and measured temperature over time are presented in Figure 4.6a. In figure 4.6b, the sensor voltage, both raw and upscaled, and the control voltage, both the reference and output. The control voltage output was mathematically converted into a duty cycle for the PWM and is presented in Figure 4.6c. The current draw over time is presented in Figure 4.6d.

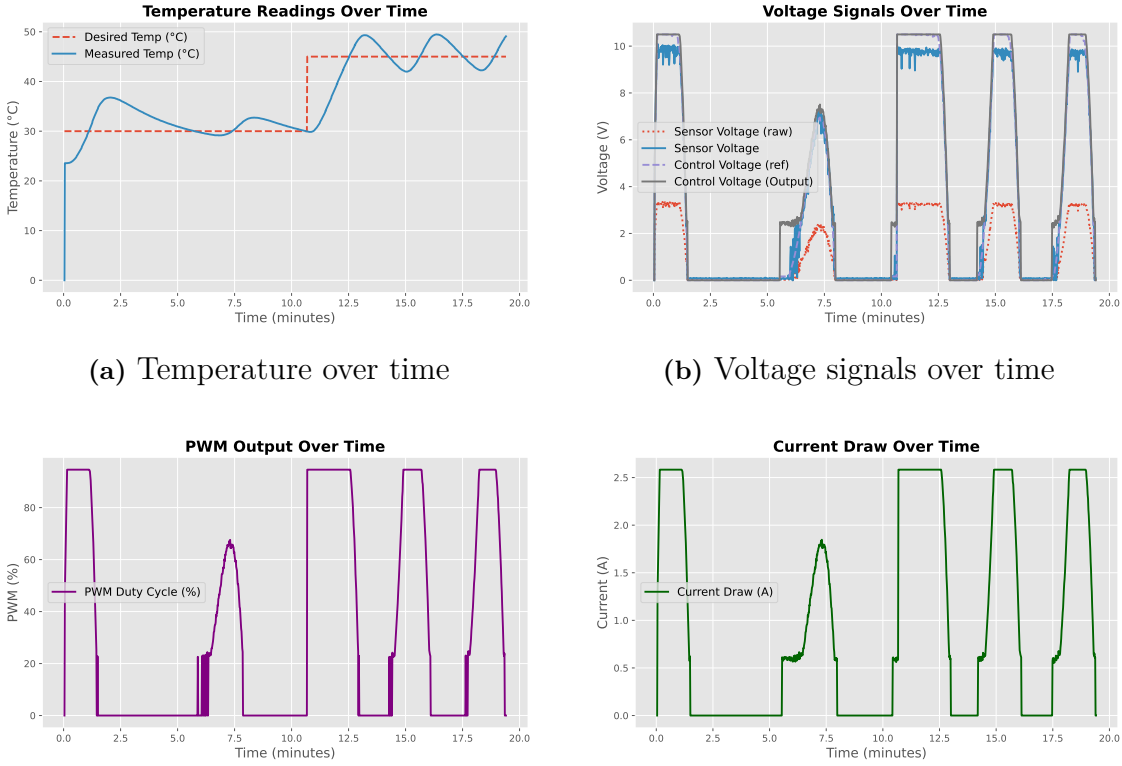


**(a)** Temperature over time

**(b)** Voltage signals over time

**(c)** PWM duty cycle

**(d)** Current draw

**Figure 4.6:** System response plots: temperature, voltage, PWM duty cycle, and current. Recorder from Arduino data points

### 4.2.5 Physical Jacket

The jacket had the pads integrated into the lining of the jacket, the battery, buck and encasing for the sensor circuit were placed in the side inner pocket. The battery was placed in the back. The inside pockets can be seen in Figure 4.7. The components and weight of the battery did not obstruct the jacket's movements or wearability. The outside of the jacket can be seen in Figure 4.8

**Figure 4.7:** The battery pocket on the left picture, The user interface and buck pocket on the right picture

**Figure 4.8:** The jacket outside front and back

The system could heat and change temperature while a person had it on. Thermal pictures of the heating pads working while the jacket is worn can be seen in Figure 4.9.

**Figure 4.9:** Thermal pictures of the jacket worn front and back

## 4.3 Interpretation and Commentary on Results

This section will present and discuss the results of the tests that were carried out.

### 4.3.1 Heating element

Several different types of heating elements were initially considered. Carbon fibre was the first option, given its good electrical resistance and ability to distribute heat evenly, making it a solid choice for a heating element. However, there were some health risks associated with carbon fibre. Small fibres could detach and become airborne when working with the carbon fibre which would pose an inhalation risk. Because of this, the lab where the implementation and testing was performed, did not allow the use of carbon fibre, which ruled it out.

Tests were also performed using a silicone heater mat, which is a type of metal wire heating element. These tests, presented in Table A.1 showed promising results, demonstrating a relatively low current, which is important for both safety and battery life, and also sufficient heating for the jacket, making it a strong candidate. However, the cost of the silicone heater mat was considered unreasonably high for the project, as the jacket was not intended to be an extremely expensive product.

As an alternative and feasible cost-effective solution, it was decided to create a custom heating element using metal wire. The custom heating element included a nichrome wire, along with glass fibre insulation to protect the wire. The wire assembly is then sandwiched between protective layers to form the heating element. Although the custom-made heating element did not achieve the same level of efficiency as the silicone heating mat, it still reached a sufficient temperature to be considered viable for this project, as seen in Figure 3.1. Additionally, unlike the silicone mat, where the dimensions are not very adjustable, the custom element was incredibly adjustable and presented the opportunity to choose the length and width. This enabled a heating element design that was streamlined for this specific jacket.

A notable part of Figure 3.1 is that the temperature was much higher on the interfacing pads than any other case, being on average $20\,°C$ higher. There might be two reasons for this. The first is that measuring the temperature directly on the wires was much easier on the pads than in all other cases. The interfacing distributed the heat more evenly, making the area of heating much thicker than in the other cases. That made the heated area thicker, which made it easier to aim the laser directly at the wire. The second reason is that the interfacing pads' function is to distribute and transfer heat to a reasonable degree. That made the heat energy not transfer as fast as the metal wires; instead, it stayed on the pad more evenly, resulting in a higher temperature. This might also be the reason why the jacket did not have as high a temperature, since there is a bit of empty air between the heating pad and inner lining.

### 4.3.2 Power stage

The main part of the power stage, the buck converter, worked fine, as can be seen in the signals presented in Figures 4.1 4.2 4.3. The MOSFETs followed the duty cycle of the Arduino's PWM within 2 percentage points, although slightly delayed, due to the rise and delay times of the MOSFETs, but that should not change the resulting voltage in any case. The maximum output voltage was only barely $10\,V$ whereas it should theoretically be closer to $10.5\,V$, which implies a voltage drop across the various components in the physical hardware.

### 4.3.3 Sensing and control system

One of the major setbacks of the wires compared to other heating elements is the uneven heat distribution. As seen in Figure 3.1, the measured temperatures on different parts of the unshielded wire vary with up to $40\,°C$, and increase with higher voltages. By adding shielding and padding, this unevenness is reduced, but is still clear on the highest temperature settings. The unevenness makes it difficult to ensure the intended temperature is kept in the jacket.

The resulting controller is not entirely satisfactory. As presented in Figure 4.6, the regulatory system is slow and oscillates around the reference temperature without finding a stable point. This is because of faults in the outer loop of the control system and because of the limitations with a slow temperature sensor, relative to the controller, temperature sensor which also depends on thermal dispersion. Furthermore, no model of the heating system was created which made it hard to predict.

To make the system faster, a temperature sensor with better reaction time could be used, since this would allow for a faster regulating system. This is an economic issue since faster sensors typically are more expensive. An IR sensor could have been used, but they are not practical to use in a heated jacket. This is because they need a clear line of sight to the measurement area, something that can not be assured because of movement and other clothing.

## 4.4 Limitations of the Study

In this section the shortcomings of the project are discussed.

### 4.4.1 Heating element

During development, there were some issues regarding the wire length. It was found that if the heating wire was too long, the element would not reach a high enough temperature. Additionally, it was discovered that connecting multiple heating elements in parallel to the battery caused the current to become too high, which was not acceptable for wearable clothing. Therefore, the total length of metal wire used across all heating elements needed to be kept at $1.5\,m$ to ensure a temperature of 58 $°C$ while maintaining a safe current level. A more effective heating element could make larger and more pads possible. However, this jacket system was restricted to

only 4 smaller pads.

### 4.4.2 Control system

In the end, the control system did not function exactly as envisioned. When a target temperature was set, the Arduino would initially increase the duty cycle to a high value, allowing the temperature to ramp up quickly. Once the measured temperature approached the set value, the controller would begin adjusting the duty cycle down, effectively switching the heat on and off to try and maintain a stable temperature.

While the temperature would eventually reach the desired value, the system showed a lot of oscillations and instability when attempting to maintain the set temperature. The temperature sensor was relatively slow, it had a rise time of $5-20$ seconds. The slow change in the temperature sensor, with the addition of a relatively slow heat dispersion, meant that the control variables had the same error input for many cycles and caused the control variable to often swing between maximum and minimum duty cycles as can be seen in Figure 4.6. It is worth mentioning, however, that the temperature still was within $5\,°C$ even while these large swings were happening. When testing the jacket, a user could feel the heat elements switch on and off between the $\pm 5\,C°$. The slow rise time and unstable temperature could be irritating for the user, so the jacket has room for improvement.

It was also especially difficult for the controller to lower the temperature after being set at a higher temperature. This is mostly due to the temperature in the testing room being around $21\,°C$ and because the all-season jacket is designed to store heat, leading to little heat loss. If the jacket was tested in colder environments, the control system and heat development might give a different result.

### 4.4.3 Battery

The aim of the project was to make a jacket that could be powered for up to 8 hours before it would need to be recharged. After testing the whole system for 20 minutes, the current was deemed to be around $1\,A$ as presented in 4.6d. With a $5400\,mAh$ battery the operating time for $45\,°C$ to be more towards the 5.4 hour mark, about 2.5 hours lower than what was expected. However, this was an informed decision because this is a prototype and will not be used for more than 5 hours without having an available battery charger.

### 4.4.4 Buck-converter

The decision to build a buck instead of buying a commercial one was successful, although it was very time-consuming. The perk of building one was to be able to digitally program the duty cycle, a function most of the commercial bucks do not have. A commercial alternative, if purchased, could have been utilised, compromising on some aspects concerning programming and control design.

### 4.4.5 Usage of the jacket

Because of the jacket's thin interfacing it has some good versatility on the market. Being able to use it all winter, autumn, and spring is a positive, and is still a unique niche the market. It is however, still a very robust and heavy worker's jacket, and therefore better made for such uses. One area of development for this jacket is that it is currently not washable. The heating wires are not secured enough, and the electronics are not easily removable. If the jacket was washed, the wires could be displaced, and the electronics could take damage from the water and turbulence in the washer. Making the jacket washable was part of the scope, but since this was more of a design problem than a technical one, this was not a priority.

This section discusses the societal and ethical aspects in designing and implementing a temperature-controlled jacket.

### 4.4.6 Clothing production and consumption

The production of a jacket can be quite wasteful when it comes to emissions and energy. When it comes to common garments, a jacket releases the most emissions and is the second most energy-consuming in a life cycle[44]. On the other hand, a jacket has a lot of uses per life cycle. Using a well-made high-end jacket also has the potential to extend the lifespan of the jacket, with the price tag encouraging long-term use. A big problem is that a large number of jackets are not used like this and are quickly thrown out. A well-adapted and robust heated jacket could replace a lot of these so-called wear and tear jackets, thus reducing the jacket consumption.

### 4.4.7 Repairs and maintenance

An important part in extending the life cycle of a product is to be able to repair and perform maintenance on the product [45]. Designing a jacket for maintenance could be making it washable, while reparation would require spare parts easy to install. The battery is easily detachable, making it possible to replace it if needed. However, the rest of the system does not fulfil this goal. Making the jacket washable would require all parts of the heating system to be either waterproof or easy to remove, but this is not the case. With no way to remove the wires and components, repairing and washing the jacket is difficult. It is possible to make this improvement with the current jacket, but there was not enough time in the project's time frame. That makes the jacket's product life cycle less sustainable than otherwise possible.

### 4.4.8 Safety measures

A very important part of making the heated jacket wearable are the safety measures. If the control system fails and stops responding to commands there needs to be an easy way to turn the heating system off manually. To meet this requirement, a hardware switch is implemented that overrides the software logic and halts the circuit from operating.

## 4.5 Recommendations and Future Work

Some aspects that could be further researched are for instance, how one could implement more pads in the jacket while having the same, or better, performance and still being safe to wear. If more pads could be added, it would be interesting to see if pads around the wrist and stomach could be implemented. The wrists easily get cold because of their closer relation to the edge of the jacket and because they are relatively far from the heart. The question would then be if the pads around the wrists would need more voltage than the other pads because of their larger heat loss. Pads around the stomach would be easy to implement, but a good addition for the user. If added, they could warm the hands through the pockets of the jacket, along with adding greater comfort for the user.

One of the goals for the jacket was to make it washable. This goal was not reached, as most of the components are impossible to remove from the end product. In addition, there is little safety implemented if the jacket is drenched in water. A circuit failure in water will not pose a safety risk to the user, but it will damage the system. A solution to handling water and humidity in the jacket could be interesting to research. On the note of humidity, the current control system is only designed to take into account the temperature in the jacket, and not the humidity. The sensor in the jacket can sense the humidity, but this was not used because of time constraints. For a better control system, humidity is important, especially if the jacket is to be used while exercising.

One important step this paper has not analysed at all is the user experience. There is existing research of the experience of thermal products on the market, but none of those systems have the control this jacket offers. Aspects such as improvement on UI and control system based on response from different users could be something to look in future.

Further work could be performed on tuning the control system better and also implementing some advanced control strategies rather than having a simple PI regulator to achieve better tracking. The use of a simple PI controller as a theoretical framework to regulate the heat was not fully effective. The Arduino took input from the temperature sensors and affected the duty cycle accordingly initially, finding the desired temperature. However, after some time, the temperature started to increase above desired value. Other control systems could have been more effective, such as a PID regulator. In addition a better anti wind-up and thermal model of heat change in the prototype is also important considerations for future work.

The decision to build a buck instead of buying a commercial one was successful, although it was very time-consuming. The perk of building one was to be able to digitally program the duty cycle, a function most of the commercial bucks do not have. A commercial alternative, if purchased, could have been utilised, compromising on some aspects concerning programming and control design.

# 5

# Conclusion

In this project, a prototype of a temperature-controlled thermal jacket is developed. Different heating elements that could be used to achieve the required heating are explored, and two of them, namely silicone heating pads and nichrome heating wire, are tested. The response of the heating element with varied voltages is observed, and it was decided to proceed with the nichrome heating element, considering the cost effectiveness and flexibility in comparison with the silicone heating pad. A synchronous buck converter is designed and built to help with smooth and consistent regulation of the power delivered, thus controlling the heat produced by the heating element. An appropriate control design is implemented using the Arduino controller to achieve the desired temperature set by the user. A user interface with display and control buttons is interfaced with the Arduino to allow temperature setting by the user and display of the temperature.

# Bibliography


[1] A. Kabel, J. Dimka, and K. McBee-Black, "Clothing-related barriers experienced by people with mobility disabilities and impairments," *Applied Ergonomics*, vol. 59, pp. 165–169, 2017, ISSN: 0003-6870. DOI: https://doi.org/10.1016/j.apergo.2016.08.036.

[2] S. Fang, R. Wang, H. Ni, H. Liu, and L. Liu, "A review of flexible electric heating element and electric heating garments," *Journal of Industrial Textiles*, vol. 51, no. 1_suppl, 101S–136S, 2022. DOI: 10.1177/1528083720968278.

[3] *Gerbing heated clothing*, https://www.gerbing.com/, Accessed: 2025-02-12.

[4] B. Hemanth, M. Meghashree, S. M. B, S. P. K, and R. Kalangude, "Heating and cooling jacket for military for optimal comfort," in *2024 IEEE International Conference on Communication, Computing and Signal Processing (IICCCS)*, 2024, pp. 1–3. DOI: 10.1109/IICCCS61609.2024.10763866.

[5] R. L. S. Tan, B. Salam, and L. L. Wai, "Fabrication of coldroom apparels with flexible washable heater," in *2022 IEEE 24th Electronics Packaging Technology Conference (EPTC)*, 2022, pp. 303–306. DOI: 10.1109/EPTC56328.2022.10013160.

[6] P. De and P. Chauhan, "Protective textile using phase change material," *Asian Textile Journal*, vol. 14, no. 3, pp. 75–82, 2005. [Online]. Available: https://www.scopus.com/inward/record.uri?eid=2-s2.0-17044373557&partnerID=40&md5=ad86038dcd073e92945e72e23ab15f16.

[7] L.-S. Fan and F. Li, "Chemical looping technology and its fossil energy conversion applications," *Industrial and Engineering Chemistry Research*, vol. 49, no. 21, pp. 10 200–10 211, 2010. DOI: 10.1021/ie1005542. [Online]. Available: https://www.scopus.com/inward/record.uri?eid=2-s2.0-78049401610&doi=10.1021%2fie1005542&partnerID=40&md5=57911cbe852cfd9978e76542eb43b709.

[8] J. Liao, L. Zhang, and R. Guo, "Evaluation of thermal and wet comfort of electrically heated vest with graphene as heating material; []" in *Journal of Beijing Institute of Fashion Technology (Natural Science Edition)*, vol. 43, 2023, pp. 50–57. DOI: 10.16454/j.cnki.issn.1001-0564.2023.02.007. [Online]. Available: https://www.scopus.com/inward/record.uri?eid=2-s2.0-85189803064&doi=10.16454%2fj.cnki.issn.1001-0564.2023.02.007&partnerID=40&md5=71dc30b064cf73addf1797d80ca39e08.

[9] R. Mt Pettys-Baker, H. Woelfle, S. Antonio Fernandes, I. Mack, and L. E. Dunne, "User-controlled multi-zone jacket for thermal microclimate regulation," 2020, pp. 203–206. DOI: 10.1145/3460421.3478834. [Online]. Available: https://www.scopus.com/inward/record.uri?eid=2-s2.0-85115934821&doi=10.1145%2f3460421.3478834&partnerID=40&md5=195ffeaecb710445a037afa79978851d.

[10] S. Fang, R. Wang, H. Ni, H. Liu, and L. Liu, "A review of flexible electric heating element and electric heating garments," *Journal of Industrial Textiles*, vol. 51, no. 1, 101S–136S, 2022. [Online]. Available: https://www.scopus.com/inward/record.uri?eid=2-s2.0-85094638022&doi=10.1177%2f1528083720968278&partnerID=40&md5=c4e24b12dc0a0e30660881d2497c4bc4.

[11] A. Arabuli, S. Arabuli, O. Kyzymchuk, and L. Melnyk, "Electric heating clothing for motorcyclists," *Vlakna a Textil*, vol. 30, no. 2, pp. 43–50, 2023. [Online]. Available: https://www.scopus.com/inward/record.uri?eid=2-s2.0-85163725807&doi=10.15240%2fTUL%2f008%2f2023-2-005&partnerID=40&md5=77cdc35c8703438f0b193862a12536bc.

[12] A. Nazem Boushehri, N. Ezazshahabi, and M. A. Tehran, "Fabrication and thermal assessment of three-layer woven heating fabrics," *Journal of Industrial Textiles*, vol. 51, no. $3_s$*uppl*, 4022S–4040S, 2022. [Online]. Available: https://www.scopus.com/inward/record.uri?eid=2-s2.0-85126071593&doi=10.1177%2f1528083721079272&partnerID=40&md5=891f1349f0950e69565db821b7dc74bd.

[13] A. Katunin, O. Kulakov, O. Roianov, and Y. Mykhailovska, "Investigation the intensity of heating of the isolation material of an electrical wire," *Materials Science Forum*, vol. 1126, pp. 143–150, 2024. [Online]. Available: https://www.scopus.com/inward/record.uri?eid=2-s2.0-85206119009&doi=10.4028%2fp-1Q1WUp&partnerID=40&md5=79e6476e282a26b8b31415a223c80597.

[14] *Silicone Heater Mat*, Corby, United Kingdom: RS Components, 2024, [Online]. Available: https://docs.rs-online.com/78bf/A700000008849882.pdf, Accessed on: 2025-04-29.

[15] *HellermannTyton Braided Fibreglass Natural Cable Sleeve*, Crawley, United Kingdom: HellermannTyton, 2020, [Online]. Available: https://docs.rs-online.com/39df/0900766b817079d1.pdf, Accessed on: 2025-05-09.

[16] S. Neves, S. Couto, J. Campos, and T. Mayor, "Advances in the optimisation of apparel heating products: A numerical approach to study heat transport through a blanket with an embedded smart heating system," *Applied Thermal Engineering*, vol. 87, pp. 491–498, 2015, Cited by: 19; All Open Access, Green Open Access. DOI: 10.1016/j.applthermaleng.2015.05.035. [Online]. Available: https://www.scopus.com/inward/record.uri?eid=2-s2.0-84930668012&doi=10.1016%2fj.applthermaleng.2015.05.035&partnerID=40&md5=0f229973b20ced1a03a2ee6f33a5590f.

[17] T. W. P. V. Böckh, *Heat Transfer Basics and Practice*. Springer, 2011. DOI: 10.1007/978-3-642-19183-1.

[18] H. J. Lee and D. Choi, "Fabrication of heat-generating polyester through formation of conductive silver nanowire network," *Korean Journal of Metals and Materials*, vol. 62, no. 8, pp. 639–644, 2024. DOI: 10.3365/KJMM.2024.62.8.639.

[19] J. M. G. B. J. Goodno, *Mechanics of materials*. Cengage, 2021.

[20] T. Ma, L. Qi, N. Wang, and R. Jia, "Development and application of sheet-like flexible carbon fiber heat-generating element," 2014, pp. 663–666. [Online]. Available: https://www.scopus.com/inward/record.uri?eid=2-s2.0-84928018064&doi=10.2991%2fmeic-14.2014.148&partnerID=40&md5=bd5f5a85b1086c8fa41cf2739c499de7.

[21] F. Wang, Y. Liu, J. Yu, Z. Li, and B. Ding, "Recent progress on general wearable electrical heating textiles enabled by functional fibers," *Nano Energy*, vol. 124, 2024. [Online]. Available: https://www.scopus.com/inward/record.uri?eid=2-s2.0-85188030346&doi=10.1016%2fj.nanoen.2024.109497&partnerID=40&md5=cfc340a187686a5e186fa6d05d82ba53.

[22] N. Vaneeswari and J. Sakthivel, "High performance carbon fiber composite and its applications," *Man-Made Textiles in India*, vol. 51, no. 12, 2023. [Online]. Available: https://www.scopus.com/inward/record.uri?eid=2-s2.0-85181487307&partnerID=40&md5=f4c901d2ec1e22100efa1ceee10e366b.

[23] D. Bernstein, V. Castranova, K. Donaldson, *et al.*, "Testing of fibrous particles: Short-term assays and strategies - report of an ilsi risk science institute working group," *Inhalation Toxicology*, vol. 17, no. 10, pp. 497–537, 2005. [Online]. Available: https://www.scopus.com/inward/record.uri?eid=2-s2.0-23844471329&doi=10.1080%2f08958370591001121&partnerID=40&md5=da4ce7eafd5f0d6dfeecc111a7bbe7c8.

[24] RS Components, *Rs pro silicone heater mat, 7.5 w, 50 x 150mm, 12 v dc*, [Online]. Available: https://se.rs-online.com/web/p/heater-pads/0245556?gb=s (accessed on: 2025-05-12), 2025.

[25] T. Robin, "Li-polymer enables product distinction," *Power Electronics Technology*, vol. 37, no. 8, 2011. [Online]. Available: https://www.scopus.com/inward/record.uri?eid=2-s2.0-84857612145&partnerID=40&md5=307c28b219d57494282aabf132e3b0ad.

[26] N. Varan, P. Merghes, N. Plesu, L. Macarie, G. Ilia, and V. Simulescu, "Phosphorus-containing polymer electrolytes for li batteries," *Batteries*, vol. 10, no. 2, 2024. [Online]. Available: https://www.scopus.com/inward/record.uri?eid=2-s2.0-85185827560&doi=10.3390%2fbatteries10020056&partnerID=40&md5=868d460ce69a928b6b7a3513a3a8c7cd.

[27] Y. Kobayashi and K. Shono, *Lithium Batteries – Lithium Secondary Batteries – Lithium All-Solid State Battery | Solid Polymer Electrolyte Cells*. 2024, vol. 4, V4:614–V4:623. [Online]. Available: https://www.scopus.com/inward/record.uri?eid=2-s2.0-105000571016&doi=10.1016%2fB978-0-323-96022-9.00059-1&partnerID=40&md5=1cc38eec5b93e38911ff782d2af3bbe2.

[28] N. I. for Occupational Safety and Health, "Worker deaths by electrocution : A summary of niosh surveillance and investigative findings," *DHHS (NIOSH)*, vol. 98-131, 1998.

[29] N. Mohan, T. M. Undeland, and W. P. Robbins, *Power Electronics: Converters, Applications, and Design*, 3rd. John Wiley & Sons, 2002, ISBN: 0-471-42908-2.

[30] D. Butnicu, D. O. Neacsu, and A. Cracan, "A study of switching frequency impact on reliability of dc-dc pol converters with discrete transistors," *IEEE Transactions on Industry Applications*, vol. 59, no. 5, pp. 6373–6383, 2023, Cited by: 5. DOI: 10.1109/TIA.2023.3291675. [Online]. Available: https://www.scopus.com/inward/record.uri?eid=2-s2.0-85164425469&doi=10.1109%2fTIA.2023.3291675&partnerID=40&md5=03da238bfb691cc4dfc299e420b15a4f.

[31] Z. Zhang, W. Eberle, P. Lin, Y.-F. Liu, and P. C. Sen, "A new hybrid gate drive scheme for high frequency buck voltage regulators," Cited by: 9, 2008, pp. 2498–2504. DOI: 10.1109/PESC.2008.4592316. [Online]. Available: https://www.scopus.com/inward/record.uri?eid=2-s2.0-52349089281&doi=10.1109%2fPESC.2008.4592316&partnerID=40&md5=5cd7fe2e237622038b7e125685c21

[32] *LM35 Precision Centigrade Temperature Sensors*, Dallas, TX, USA: Texas Instruments, 2017, [Online]. Available: https://docs.rs-online.com/abdd/A700000006857169.pdf, Accessed on: 2025-05-12.

[33] K. J. Åström and T. Hägglund, *Advanced PID Control*. Research Triangle Park, NC: International Society of Automation (ISA), 2006, ISBN: 978-1-55617-942-6. [Online]. Available: https://app.knovel.com/hotlink/toc/id:kpAPIDC001/advanced-pid-control/advanced-pid-control.

[34] Venustas, *How many watts does a heated jacket use?* United States: Venustas, 2023. [Online]. Available: https://venustasofficial.com/blogs/news/how-many-watts-does-a-heated-jacket-use?srsltid=AfmBOoqDhHQ1SAGCFwN4EMIGC7SvOZnTztFfHLeRZOR6xXLUIaMQn, Accessed on: 2025-05-12.

[35] Fluke, *Fluke ir 62 max+ data sheet*, [Online]. Available: https://dam-assets.fluke.com/s3fs-public/6008893_0000_ENG_A_W.PDF?VersionId=q0VkYBLB3ZfwFjyNBqujB4.5r1F9nlOZ (accessed on: 2025-05-12).

[36] Arduino, *Arduino uno rev 4 wifi*, [Online]. Available: https://docs.rs-online.com/26d8/A700000010377841.pdf,

[37] J. Kamala, V. Janarthanan, and K. Santhosh, "Power mosfet based photovoltaic battery charger analysis and implementation," *International Journal of Circuits, Systems and Signal Processing*, vol. 9, pp. 33–39, 2015, Cited by: 0. [Online]. Available: https://www.scopus.com/inward/record.uri?eid=2-s2.0-84926457247&partnerID=40&md5=f364bc2778d3085e7f02e28dedf21193.

[38] Infineon, *Infineon hexfet n-channel mosfet, 47 a, 55 v, 3-pin to-220ab irlz44npbf*, El Segundo, CA, USA: Infineon, 2003. [Online]. Available: https://docs.rs-online.com/de24/0900766b807913d7.pdf, Accessed on: 2025-05-12.

[39] *IR2184 driver IC*, El Segundo , CA, USA: Infineon, 2006, [Online]. Available: https://docs.rs-online.com/9362/A700000009550103.pdf, Accessed on: 2025-05-12.

[40] C. H. Chang, C. M. Wang, C. K. Ho, W. B. Su, and H. S. Yu, "Fiberglass dermatitis: A case report," in *Kaohsiung J Med Sci*, vol. 12(8), 1996.

[41] Westinghouse, *Heated blanket silky flannel*, (accessed May. 11. 2025). [Online]. Available: https://westinghouse.com/products/heated-blanket-charcoal.

[42] M. M. Leverette, *How to select the right iron settings for any fabric*, (accessed May. 11. 2025). [Online]. Available: https://www.thespruce.com/select-correct-ironing-temperature-for-fabrics-2146186.

[43] *ChipCap 2-SIP Humidity and Temperature Sensor*, Fremont, CA, USA: Amphenol Advanced Sensors, 2018, [Online]. Available: https://docs.rs-online.com/5f02/A700000007241520.pdf, Accessed on: 2025-05-12.

[44] G. Sandin, S. Roos, B. Bahareh, Zamani, and G. Peters, "Environmental assessment of swedish clothing consumption," *mistra future fashion*, vol. 05, 2019.

[45] H. Goworek, L. Oxborrow, S. Claxton, A. McLaren, T. Cooper, and H. Hill, "Managing sustainability in the fashion business: Challenges in product development for clothing longevity in the uk," *Journal of Business Research*, vol. 117, pp. 629–641, 2020, All Open Access, Green Open Access. DOI: 10.1016/j.jbusres.2018.07.021. [Online]. Available: https://www.scopus.com/inward/record.uri?eid=2-s2.0-85051021899&doi=10.1016%2fj.jbusres.2018.07.021&partnerID=40&md5=9d492b5e7610bd2ce2fec20d03d022ec.

# A

# Appendix

## A.1 Silicone heat mat

Tests were performed on a silicone heat mat, a metal wire heating element embedded in silicone rubber as an insulation material. The current and temperature was recorded after one minute of operation when the heating mat was supplied different voltage levels. The purpose of the tests was to determine if the silicone heat mat could reach a sufficient temperature while maintaining an acceptable current. The results of these tests can be seen in Table A.1.

**Table A.1:** Voltage, current, and temperature after 1 minute of operating.

| Voltage (V) | Current (mA) | Temperature (°C) |
|---|---|---|
| 4.8 | 263 | 27 |
| 6.0 | 328 | 29 |
| 7.2 | 393 | 32 |
| 8.4 | 458 | 35 |
| 9.6 | 527 | 39 |
| 10.8 | 584 | 43 |
| 12.0 | 647 | 45 |
| 13.2 | 689 | 47 |
| 14.4 | 794 | 49 |
| 15.6 | 860 | 52 |
| 16.8 | 918 | 57 |
| 18.0 | 987 | 62 |

## A.2 Arduino Code

```
#include <SPI.h>
#include <Adafruit_GFX.h>
#include <Adafruit_ST7735.h>
// Be sure to install Adafruit seesaw library!
#include <Adafruit_seesaw.h>
#include <Adafruit_TFTShield18.h>
#include "pwm.h"
#include <Wire.h>
```

```
9
10 Adafruit_TFTShield18 ss;
11 // Display pin declaration
12 #define SD_CS 4
13 #define TFT_CS  10  // Chip select line for TFT display on
   Shield
14 #define TFT_DC   8  // Data/command line for TFT on Shield
15 #define TFT_RST  -1 // Reset line for TFT is handled by
   seesaw!
16 PwmOut pwm(D2);
17 Adafruit_ST7735 tft = Adafruit_ST7735(TFT_CS, TFT_DC, TFT_RST
   );
18
19 // Timing constants
20 static long lastMicros = micros();
21 static long lastMillis = millis();
22 static long logstatus_millis = millis();
23 const unsigned long interval = 20;          // 20 us = 50 kHz
    control update rate
24 const unsigned long interval_sensor = 150;  // 200 ms = 0.2 s
    sensor update rate
25 const unsigned long interval_logstatus = 1000; // 5 s log
   interval
26
27 bool headerPrinted = false;
28
29 // Controller gains and sample times
30 float kp = 0.116;
31 float ki = 4172.162;
32 float T = 20e-06;
33
34 int tau = 5;
35 float dead_time = 0;
36 float lambda = tau*0.25;
37 float k_process = 6.1; // deg/voltage
38 float T_sensor = 0.15; // s
39
40 // Derived gains for outer loop
41 float k = tau / (k_process * (dead_time + lambda));
42 float kp_sensor = k;
43 float ki_sensor = k/tau;
44
45 // Actuator limits
46 float Vin = 11.1;
47 const float max_V = 10.5;
48 const float min_V = 0;
49
50
51 // Tustin coefficients
```

```
52 float a = kp + (ki * T) / 2;
53 float b = -kp + (ki * T) / 2;
54 float a_sensor = kp_sensor + (ki_sensor * T_sensor) / 2;
55 float b_sensor = -kp_sensor + (ki_sensor * T_sensor) / 2;
56
57 // Application variables
58 int desiredTemp = 30;
59 static float desiredV = 0;
60 float sensorTemp = 0;
61 static float controlV = 0;
62 float pulse = 0.0;
63 int sensorValue_4_resistor;
64 bool toWarm;
65 int error = -1;
66 const float TEMP_MAX = 70;
67
68 // Button debounce
69 const unsigned long BUTTON_DEBOUNCE_MS = 100;
70 static unsigned long lastButtonMillis = 0;
71 static int lastDisplayedTemp = -1;
72
73 void setup() {
74   Wire.begin();
75   Wire.setClock(400e+3);
76   Serial.begin(9600);
77   if (!headerPrinted) {
78     Serial.println("time_ms,desiredTemp,measuredTemp,
         sensor_voltage,desiredV,controlV,measuredV,pwmPerc,
         error");
79     headerPrinted = true;
80   }
81   initTftChip();
82   initdisplayDesign(desiredTemp);
83   lastDisplayedTemp = desiredTemp;
84   for (int32_t i = TFTSHIELD_BACKLIGHT_OFF; i <
       TFTSHIELD_BACKLIGHT_ON; i += 100) {
85     ss.setBacklight(i);
86     delay(2);
87   }
88   pwm.begin(50e+3f, 0.0f);
89   pwm.pulse_perc(0.0f);
90   lastMicros = micros();
91   lastMillis = millis();
92 }
93
94 void logStatus() {
95   Serial.print(millis()); Serial.print(',');
96   Serial.print(desiredTemp); Serial.print(',');
97   Serial.print(sensorTemp, 2); Serial.print(',');
```

```
98    float rawV = sensorValue_4_resistor * (5.0 / 1023.0);
99    Serial.print(rawV, 3); Serial.print(',');
100   float measV = rawV * 3.0;
101   Serial.print(desiredV, 3); Serial.print(',');
102   Serial.print(controlV, 3); Serial.print(',');
103   Serial.print(measV, 3); Serial.print(',');
104   Serial.print(pulse, 1); Serial.print(',');
105   Serial.println(error);
106 }
107
108 void loop() {
109   if (millis() - logstatus_millis >= interval_logstatus) {
110     logstatus_millis = millis();
111     logStatus();
112   }
113   if (millis() - lastMillis >= interval_sensor) {
114     lastMillis = millis();
115     readSensor();
116     desiredV = pi_temp(sensorTemp, desiredTemp);
117   }
118   if (micros() - lastMicros >= interval) {
119     lastMicros = micros();
120     sensorValue_4_resistor = analogRead(A0);
121     float sensorV = sensorValue_4_resistor * (5.0 / 1023.0) *
          3.0;
122     controlV = pi(sensorV, desiredV);
123     toWarm = (sensorTemp > TEMP_MAX + 2 || error != 0);
124     //Serial.println(toWarm);
125     if (toWarm) {
126       pulse = 0;
127       pwm.pulse_perc(0.0f);
128     } else {
129       if (controlV > max_V) {
130         pulse = (max_V / Vin) * 100;
131         pwm.pulse_perc(pulse);
132       } else if (controlV < 2.5) {
133         pulse = 0;
134         pwm.pulse_perc(pulse);
135       } else {
136         pulse = (controlV / Vin) * 100;
137         pwm.pulse_perc(pulse);
138       }
139     }
140   }
141   handleButtons();
142 }
143
144 void readSensor() {
145   unsigned int data[4];
```

```
146   Wire.beginTransmission(0x28);
147   error = Wire.endTransmission();
148   if (error == 0) {
149     Wire.requestFrom(0x28, 4);
150     if (Wire.available() == 4) {
151       Wire.read();
152       Wire.read();
153       data[2] = Wire.read();
154       data[3] = Wire.read();
155
156       sensorTemp = (((data[2] * 256) + (data[3] & 0xFC)) / 4)
              / 16384.0 * 165.0 - 40.0;
157       //error = 0;
158     }
159   }
160 }
161
162 void handleButtons() {
163   unsigned long now = millis();
164   if (now - lastButtonMillis < BUTTON_DEBOUNCE_MS) return;
165   lastButtonMillis = now;
166   uint32_t buttons = ss.readButtons();
167   bool changed = false;
168   if (!(buttons & TFTSHIELD_BUTTON_DOWN) && desiredTemp > 30)
          { desiredTemp--; changed = true; }
169   if (!(buttons & TFTSHIELD_BUTTON_UP)   && desiredTemp < 58)
          { desiredTemp++; changed = true; }
170   if (!(buttons & TFTSHIELD_BUTTON_1)) { desiredTemp = 30;
        changed = true; }
171   if (!(buttons & TFTSHIELD_BUTTON_2)) { desiredTemp = 45;
        changed = true; }
172   if (!(buttons & TFTSHIELD_BUTTON_3)) { desiredTemp = 58;
        changed = true; }
173   if (changed && desiredTemp != lastDisplayedTemp) {
174     displayDesign(desiredTemp);
175     lastDisplayedTemp = desiredTemp;
176   }
177 }
178
179 void initTftChip() {
180   pinMode(TFT_CS, OUTPUT); digitalWrite(TFT_CS, HIGH);
181   pinMode(SD_CS, OUTPUT);  digitalWrite(SD_CS, HIGH);
182   if (!ss.begin()) while (1);
183   ss.setBacklight(TFTSHIELD_BACKLIGHT_OFF);
184   ss.tftReset();
185   tft.initR(INITR_BLACKTAB);
186 }
187
188 void initdisplayDesign(int temperature) {
```

```
189   tft.fillScreen(ST77XX_BLACK);
190   tft.setTextColor(ST77XX_WHITE);
191   tft.setRotation(1);
192   tft.setTextSize(2);
193   tft.setCursor(1, 5);
194   tft.print("Temperature");
195   tft.drawLine(0, 25, 180, 25, ST77XX_WHITE);
196   tft.fillCircle(135, 51, 8, ST77XX_WHITE);
197   tft.fillCircle(135, 51, 4, ST77XX_BLACK);
198   tft.setTextSize(7);
199   tft.setCursor(40, 50);
200   tft.print(temperature);
201   tft.setTextColor(ST77XX_WHITE, ST77XX_BLACK);
202 }
203
204 void displayDesign(int temperature) {
205   tft.setTextSize(7);
206   tft.setCursor(40, 50);
207   tft.print(temperature);
208 }
209
210 float pi(float sensorV, float desiredV) {
211     static float prev_error   = 0.0f;
212     static float prev_control = 0.0f;
213     float error   = desiredV - sensorV;
214     float delta   = a * error + b * prev_error;
215     float u_unsat = prev_control + delta;
216     float u_sat   = constrain(u_unsat, min_V, max_V); //
          clamp to actual max
217     bool withinRange  = (u_sat == u_unsat);
218     bool backIntoLow  = (u_sat == 0.0f    && delta >  0.0f);
219     bool backIntoHigh = (u_sat == max_V    && delta <  0.0f);
          // use max_V, not Vin
220     if (withinRange || backIntoLow || backIntoHigh) {
221       prev_control = u_sat;
222       prev_error   = error;
223     }
224     //Serial.println(u_sat);
225     return u_sat;
226 }
227
228 float pi_temp(float sensorTemp, float desiredTemp) {
229     const float a_s  = a_sensor;
230     const float b_s  = b_sensor;
231     const float Umax = max_V;
232     const float Umin = min_V;
233     static float prev_u     = 0.0f;
234     static float prev_error = 0.0f;
235     float error  = desiredTemp - sensorTemp;
```

```
236     //if (abs(error) < 0.25){
237     //  error=0;
238     }
239     float delta  = a_s * error + b_s * prev_error;
240     float u_unsat = prev_u + delta;
241     float u_sat   = constrain(u_unsat, Umin, Umax);
242     bool withinRange  = (u_sat == u_unsat);
243     bool backIntoLow  = (u_sat == Umin && delta >  0.0f);
244     bool backIntoHigh = (u_sat == Umax && delta <  0.0f);
245     if (withinRange || backIntoLow || backIntoHigh) {
246         prev_u     = u_sat;
247         prev_error = error;
248     }
249     //Serial.println(u_sat);
250     return u_sat;
251 }
```

**Listing A.1:** Code of Arduino

**DEPARTMENT OF ELECTRICAL ENGINEERING**
**CHALMERS UNIVERSITY OF TECHNOLOGY**
Gothenburg, Sweden
www.chalmers.se


CHALMERS